

UNIVERSITÀ DEGLI STUDI DI
NAPOLI
“FEDERICO II”



FACOLTÀ DI BIOLOGIA

Dottorato di Ricerca in Biologia
XXXIII Ciclo

“POLIFENOLI DA SEMI DI UVA: NUOVE
MOLECOLE PER L’INDUSTRIA
NUTRACEUTICA”

Tutor:
Prof. Salvatore Cozzolino
Dr. Stefania Crispi

Candidato:
Francesco Di Meo



Summary

INTRODUCTION.....	4
AIM	12
CHAPTER 1	16
MATERIALS AND METHODS	17
2.1. CELL CULTURE	17
2.2. PLANT MATERIAL.....	18
2.3. EXTRACT PREPARATION.....	18
2.4. CELL PROLIFERATION ASSAY	18
2.5. COLONY FORMING ASSAY.....	19
2.6. WOUND HEALING ASSAYS.....	19
2.7. APOPTOSIS DETECTION BY FLOW CYTOMETRY ANALYSIS	20
2.8. RNA EXTRACTION AND EXPRESSION ANALYSIS OF APOPTOTIC PATHWAY GENES IN MM CELLS.....	20
2.9. CYTOCHROME C RELEASE.....	22
2.10. WESTERN BLOT.....	22
2.13. STATISTICAL ANALYSIS.....	23
2.14. MICRO-ARRAY ANALYSIS	23
2.15. PATHWAY AND NETWORK ANALYSIS BY IPA.	24
2.16. OIL PREPARATION.....	24
RESULTS.....	26
3.1. SEED RATHER THAN PEEL EXTRACTS DETERMINE CANCER GROWTH INHIBITION	26
3.2. FGS AND AGS IMPAIR MESOTHELIOMA TUMORIGENIC PROPERTIES AFFECTING CELL PROLIFERATION AND MIGRATION	28
3.3. FGS AND AGS INDUCE APOPTOSIS IN MESOTHELIOMA CELL LINES.....	32
3.4. FGS AND AGS ACTIVATE SPECIFIC PATHWAYS INVOLVED IN APOPTOSIS	34
3.5. FGS AND AGS EXTRACTS INDUCE PROTEIN EXPRESSION OF CLEAVED PARP AND BAX AND CYTOCHROME C RELEASE.....	35
3.6. METABOLOMICS AND TRANSCRIPTOMIC ANALYSIS OF GRAPE PEEL AND SEED SAMPLES.....	38
3.7. MICROARRAY ANALYSIS	40



UNIONE EUROPEA
Fondo Sociale Europeo



3.8. AGS AND GRAPE SEED OIL DETERMINE GROWTH INHIBITION IN MESOTHELIOMA AND BREAST CANCER CELLS.	43
3.9. AGS AND GRAPE SEED OIL BIOACTIVITY ON MESOTHELIOMA AND BREAST CANCER CELLS.	45
3.10. AGS BIOACTIVITY ON MEDULLOBLASTOMA CELLS	48
3.11. PROTEIN EXPRESSION ANALYSIS	50
DISCUSSION	53
CHAPTER 2	59
MATERIALS AND METHODS	60
4.1. CELL CULTURE AND CHEMICALS	60
4.2. CELL PROLIFERATION ASSAY	60
4.3. PROPIDIUM IODIDE AND DAPI STAINING ASSAY	61
4.4. MITOCHONDRIA MEMBRANE POTENTIAL MEASUREMENT	61
4.5. RNA EXTRACTION AND Q-PCR	62
4.6. WESTERN BLOT	63
4.7. STATISTICAL ANALYSIS	63
RESULTS	65
5.1. EGB PROTECTS SK-N-BE CELLS AGAINST OXIDATIVE STRESS INDUCED APOPTOTIC CELL DEATH. ..	65
5.2. EGB PROTECTS SK-N-BE CELLS AGAINST OXIDATIVE STRESS INDUCED APOPTOSIS	69
5.3. EGB MITIGATED THE H₂O₂ INDUCED DECREASE IN MITOCHONDRIAL MEMBRANE POTENTIAL	71
5.4. EGB EXHIBITS INTRACELLULAR ANTI-APOPTOTIC EFFECT	73
DISCUSSION	75
CONCLUSION	78
REFERENCES	80
DOTT. FRANCESCO DI MEO PEER REVIEWED PAPERS PUBLISHED DURING THE PHD PERIOD:	91



UNIONE EUROPEA
Fondo Sociale Europeo



Introduction

In the recent years there is a growing industrial interest in the recovery and reuse of waste from production processes in the food industry. Industrial and agro-industrial by-products and waste can be recovered and valorised, transforming them into new materials and products with high added value. Industrial and agro-industrial waste are enhanced through their reuse in the preparation of innovative materials and components.

In fact, to date the deficiency of natural resources, climate change, food loss and waste are decreasing the availability of food and raw materials. Decline of natural resources worldwide, degradation in land, water and biodiversity, poses questions about the ability to meet food and material demands for the next future. Consequently, finding the balance between the increasing demand for resources and sustainable supply is the challenge of the present and the future.

Food supply chains start with agricultural phase, continue with manufacturing, retail and end with consumption. Throughout this cycle, food is lost or wasted because of a variety of reasons, i.e., technical, economic or social problems.

In the twentieth century, the prevalent policy was to increase food production but not to improve the efficiency of the food production system. Food loss or waste were not considered a problem. Only in the 21th century, the increased demand for food, the depletion of natural resources, the restrict energy demands and the minimize of economic costs have led to this problem.



UNIONE EUROPEA
Fondo Sociale Europeo



Food processing industries generate an impressive amount of waste, consisting especially of the organic residues of processed raw materials. Most of these materials, defined waste, could represent an added value. The same term “waste” indicates a wide variety of products coming out of the production system. In fact, lately, the new term “waste by-products”, indicating products that can be reused, is gaining popularity. The possibility to recover by-products from production processes is very wide and varied and depends on the type of process under consideration. For example, vegetable by-products and plant residues, due to their content of polyphenols, glucosinolates, proteins, pectin, phytochemicals and plant enzymes, may be used to generate innovative products such as dietary fibres, food flavours or food supplements.

Thus, in recent years, the concept of circular economy has become more and more established. Circular economy is a term that defines an economic system designed to be able to regenerate itself, therefore guaranteeing its eco-sustainability. The principal aim is the waste reduction and the reuse of resources.

Wineries constitute one of the most important agro-industrial sectors worldwide. Grapes are one of the most cultivated fruits worldwide, with the production of more than 60 million metric tons per year. *Vitis vinifera* is the most commonly cultivated species for wine production, and according to the FAO, around 80% of its production represents 78 million tons that has been used in the wine sector. Winemaking process generates an ample variety of solid and liquid by-products, including vine shoots, grape marc or grape pomace, wine lees, spent filter cakes, vinasses, and winery wastewater that



UNIONE EUROPEA
Fondo Sociale Europeo



must be treated, disposed of or reused properly, in order to avoid negative environmental impact. Large quantities of scraps are composed of rejected or inedible plant tissues with a high amount of water content and organic matter. Therefore, special attention has been given to more advantageous and sustainable options by both the scientific community and the producers, aiming at maximum utilization of all raw materials and by-products derived from the wine industry, ultimately reducing to a minimum the disposal of waste streams.

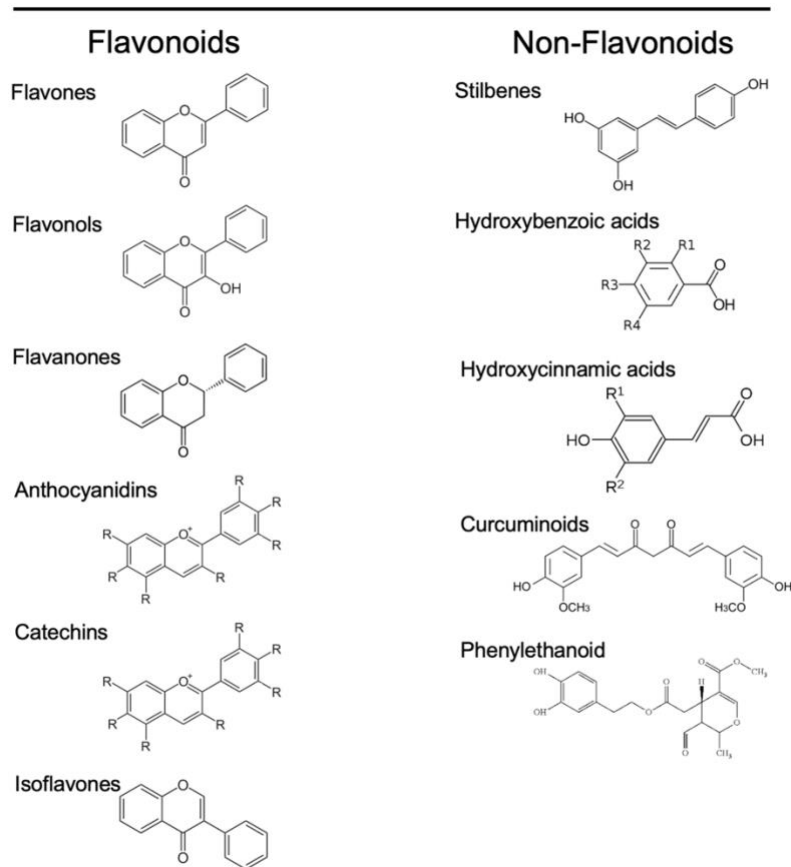
Since ancient times and particularly in Mediterranean countries, wine has been closely associated with the diet, and its regular consumption has been associated with health benefits. Epidemiological and clinical studies around the world, over the past twenty years, have pointed out that the moderate intake of alcoholic beverages produces positive effects on antioxidant capacity, lipid profile and the coagulation system. Several studies have focused their attention on the components of red wine (mainly polyphenols and especially resveratrol) since the so-called “French paradox” was first described. Although the chemical constituents of grapes and wine may vary, similar beneficial effects have been observed in different varieties of red wine related to their higher polyphenolic content. Among food industry wastes, grape wastes are partially used in cosmeceutical and nutraceutical fields. However, little is known about the potential use of grape seeds. In fact, if the use of pulp and skin of grapes is already widely spread, the properties of grape seeds are not well characterized yet. Grapevine (*Vitis vinifera* L.) is a plant rich of bioactive compounds that are principally distributed in berry skin, stem, leaves and seeds, rather than in the pulp of the berry. Among the



substances accumulated in grapes, the most important and biologically interesting ones are surely polyphenols. About 70% of the polyphenols contained in grapes are present in the grape seed.

Polyphenols are the most abundant secondary metabolites present in the plant kingdom. They represent a large and diverse group of molecules including two main families, the flavonoids and the non-flavonoids. Plant polyphenols belong to different groups: phenolic acids, phenolic diterpenes, volatile oils, flavonoids and stilbenes. All of them are characterized by multiples of phenol units.

Polyphenols





UNIONE EUROPEA
Fondo Sociale Europeo



Figure 1.1 Structures of polyphenols. Polyphenols are classified by the number of phenol rings in flavonoids and non-flavonoids. The figure shows basic skeleton structure of polyphenols. Image from: [1]

Polyphenols are known for their anti-inflammatory, antimicrobial and antioxidant activities and are of interest in nutraceutical and cosmetic fields [1-3]. Moreover, some of them can also have cytotoxic effects and therefore they can be studied to develop new molecules with pharmacological activity. Polyphenols present in higher quantities in grapes are mainly flavonoids (anthocyanins, flavanols and flavonols), stilbenes and phenolic acids [4]. Anthocyanins and flavonols are mainly found in the skin [5] whereas flavanols and hydroxycinnamic derivatives (among the most common ones we find coumaric acid, caffeic acid and ferulic acid) have been found in higher quantities in grape seeds [6].

Anthocyanins are the main polyphenols in red grapes, whereas flavan-3-ols are more abundant in the white variety [7].

Anthocyanins belong to the flavonoid family. These molecules consist of a benzene molecule fused with a pyran molecule, linked with a phenyl group that can be in turn linked to several substituents.

Anthocyanins are polyhydroxylated polyaromatic compounds capable of reacting with oxidants such as molecular oxygen and free radicals thus reducing the damage that these molecules can cause to cells and tissues [8].

Flavan-3-ols are derivatives of flavans that possess a 2-phenyl-3,4-dihydro-2H-chromen-3-ol skeleton. These compounds include catechin, epicatechin gallate, epigallocatechin, epigallocatechin gallate, and proanthocyanidins [9].



UNIONE EUROPEA
Fondo Sociale Europeo



However, the effects of polyphenols are often limited by their poor bioavailability [10]. Moreover, *in vivo* studies the dosage of single molecules of polyphenols did not have the expected effect. This can be due to the limited absorption but also to the lack of a synergistic action among the various molecules composing an extract [11].

For this reason, bioactive phytochemicals taken through diet represent a promising opportunity for the development of more effective strategies for the prevention or treatment of cancers that can be utilized as complementary to traditional medicine.

For thousands of years, different cultures have used phytochemicals for treatment of various diseases, nevertheless their active ingredients or mechanisms of action often are not well characterized. Grape seed extract are hopeful bioactive molecules that have demonstrated anticarcinogenic effects *in vitro* and *in vivo* analysis and exhibit no toxicity *in vitro* [12,13].

Phytochemicals can act also as protective agent against oxidative stress. Flavonoids are in particular described as the molecules with a strong bioactivity in brain functions with positive effects on synaptic plasticity and neuronal activity. Among the bioactive phytochemicals, *Ginkgo biloba* is one of the most used worldwide [14]. *Ginkgo biloba* fallen leaves are treated as waste to be incinerated, polluting the air, soil and rivers. In addition, the leaves have become a problem for local businesses and governments in the plantation area to dispose of [15]. Therefore, its recovery to produce nutraceutical extracts may be a solution to this problem. *Ginkgo biloba* has been widely used in the treatment of cardiovascular and cerebrovascular diseases, liver cirrhosis and acute and chronic renal disease. More recently, a



UNIONE EUROPEA
Fondo Sociale Europeo



standardized extract of *Ginkgo biloba*, EGb 761, has been found to have neuroprotective effects in several central nervous system and neurodegenerative diseases [14]. EGb 761 (EGb) is a standardised extract of *Ginkgo biloba* leaves that contains a well-defined concentration of flavone glycosides and terpene lactones (24% and 6%, respectively). In fact, EGb contains 6% terpenoids (in which 3.1% are ginkgolides A, B, C, and J and 2.9% is bilobalide), 24% flavonoid glycosides, and 5% to 10% organic acids [16]. The flavonoids act as free radical scavenging, whereas terpenes lactones protect mitochondrial membranes from free radical damage [17]. EGb has been described to have antioxidant properties playing an important role as a free radical scavenger [18]. It has been demonstrated that the antioxidant activity, as a “radical scavenger”, is due to its superoxide dismutase-like activity that enables it to scavenge hydroxyl radicals [19]. *Ginkgo biloba* also has the capacity to regulate the oxidative stress. The levels of glutathione, malondialdehyde, superoxide dismutase and nitric oxide, increased after a treatment with EGb [20]. These properties determine beneficial effects in neurodegenerative diseases as Alzheimer [21,22] or Parkinson [23]. However, the mechanism of the action of EGb protection against oxidative stress-induced apoptosis remains to be fully elucidated.

In fact, oxidative stress is one of the main causes of neural damage. EGb 761 exerts neuroprotective action mainly acting as free radical–scavenger. In fact, EGb 761 is able to reduce the endogenous and the induced levels of ROS [24]. This activity is linked to the chemical structure of the flavonoids that allow to not only to react and directly scavenge, the hydroxyl radicals but also to inhibit the formation of new hydroxyl radicals [25].



UNIONE EUROPEA
Fondo Sociale Europeo



It is well known that oxidative stress determines the activation of the apoptotic processes, thus playing a crucial role in most of neurological diseases.

The evidence mentioned above prompted us to explore the protective effect of EGb 761 against oxidative stress-induced apoptosis in neuroblastoma cells.



UNIONE EUROPEA
Fondo Sociale Europeo



Aim

The main aim of this study was to analyse the anti-cancer potential of grape seeds global semipolar extracts of two Italian grape varieties Aglianico (red) and Falanghina (white) in cancer cell lines. Many studies have shown that extracts from different cultivar can have different efficacy. It is believed that this difference is due to a different chemical composition.

The use of natural extracts represents a new resource for the treatment of cancer, which can be used alongside the already established chemotherapy, radiotherapy and surgery.

One of the major advantages of natural products is represented by the low intensity of side effects, which are usually milder than those associated to the use of chemotherapeutics.

Initially, we tested the efficacy of the two grape seed extracts on mesothelioma cell lines. Malignant mesothelioma is a rather rare and aggressive cancer of the mesothelium, the epithelium lining vital organs such as the lungs and heart and body cavities such as the peritoneal cavity. The worldwide incidence is 2.2 cases per million population [26].

We used three mesothelioma cell lines, MSTO-221H and NCI-H2452, sensitive to standard chemotherapeutic treatment, and IST-Mes2, insensitive to chemotherapeutic treatment.

Usually, phytochemicals anticancer activities are exerted by inducing programmed cell death (apoptosis). Apoptosis can be executed through the intrinsic or the extrinsic pathway. The extrinsic pathway is activated by the bond of death receptors and their ligand, as the receptor FAS and his ligand



UNIONE EUROPEA
Fondo Sociale Europeo



FASL. The intrinsic pathway is regulated by B-cell lymphoma-2 (BCL-2) family proteins. BAX (Bcl-2-associated X protein) impairs mitochondrial membranes determining cytochrome *c* release, and this activity is inhibited by binding of BCL-2 to BAX. Unbalance between BCL-2 and BAX favours BAX activity, determining the onset of apoptosis. Therefore, we decided to analyse gene and protein expression of regulatory genes of these pathways. Once the most promising and effective extract was chosen, we analysed the transcriptional pathways modulated following treatment.

Afterward, we wanted to understand if the anticancer effects were restricted to mesothelioma only or also to other tumours.

Therefore, the effect of grape seed extract was tested in breast cancer. Breast cancer is the most common tumour in women, and one of the three most common cancers worldwide [27] and its morbidity shows an increasing trend year by year [28].

We used a cell line of breast cancer, MDA-MB-231, frequently used as late-stage breast cancer model. This cell line is ER, PR, and E-cadherin negative and expresses mutated p53 [29].

Subsequently, we tested the biological effects of grape seed extract on medulloblastoma cells. Medulloblastoma is the most common paediatric brain tumour and is currently treated by surgery, radiotherapy, and chemotherapy [30]. Although this multi-modal treatment is the most effective, the aggressive nature of this therapy results in a number of serious neurocognitive side effects. We used two different cell lines, DAOY HTB-186 and D283 Med HTB-185, which have a higher degree of stemness than the former.



UNIONE EUROPEA
Fondo Sociale Europeo



The industrial characterization of the PhD pushed us to try to understand how to industrialize the process of production of the extract, to understand the common points with the industrial processes already widely developed for the production of other derivatives from grape seeds, and the economic feasibility of the project. Following this route, we have analysed the biological effects of grape seed oil, a commercial product derived from grape seeds.

In the second chapter of this thesis, I have analysed the antioxidant potential of flavonoids present in a standardized *Ginkgo biloba* extract. In fact, oxidative stress occurs in the cell when the antioxidant defence is unable to balance the rate of the reactive oxygen species generated [31].

When present in excess, oxidants elevate the intracellular levels of reactive oxygen species (ROS) and damage cell membrane, proteins and DNA.

We chose to analyze *Ginkgo biloba* protective effects in neurons that are particularly prone to production of ROS and highly susceptible to redox stress, because of their high lipid and metal ion content combined with their high metabolic rate and relatively low concentrations of antioxidants [32]. Neuronal cell death induced by oxidative stress is especially dangerous because adult neurons are post-mitotic cells with limited capacity to proliferate or be replaced. Therefore, in neuronal cells, reduction of oxidative stress could inhibit apoptosis potentially preventing neurodegeneration.

I have analyzed the protective effect of EGb 761 on oxidative stress-induced apoptosis in SK-N-BE cells with the aim to unravel the molecular pathway in which EGb 761 acts as antioxidant. SK-N-BE is a human neuroblastoma



UNIONE EUROPEA
Fondo Sociale Europeo



cell line, commonly used as cellular model for research studies aimed to analyze the role of oxidative stress in neurodegeneration [33-35].



UNIONE EUROPEA
Fondo Sociale Europeo



Chapter 1

Polyphenols from grape seed extract



UNIONE EUROPEA
Fondo Sociale Europeo



Materials and Methods

2.1. Cell culture

Human malignant mesothelioma cell lines MSTO-221H (MSTO) and NCI-H2452 (NCI) were grown in RPMI supplemented with 10% FBS, glutamine (2 mM), sodium pyruvate and antibiotics (0.02 IU/mL-1 penicillin and 0.02 mg/mL-1 streptomycin). Human mesothelioma cells Ist-Mes2 (Mes2) were cultured in DMEM, supplemented with 10% FBS, glutamine (2mM), 1% nonessential amino acids, and antibiotics (0.02 IU/mL-1 penicillin and 0.02 mg/mL-1 streptomycin).

Human mesothelium cell lines, Met5-A, were grown in RPMI supplemented with 10% FBS, glutamine (2 mM), sodium pyruvate and antibiotics (0.02 IU/mL-1 penicillin and 0.02 mg/mL-1 streptomycin).

Human breast adenocarcinoma cell line MDA-MB-231(MDA) were maintained in RPMI 1640 medium supplemented with 10% FBS.

The human mammary epithelial cell line, MCF10A cells, were cultured in DMEM/Ham's F-12 supplemented with 100 ng/ml cholera toxin, 20 ng/ml epidermal growth factor, 0.01 mg/ml insulin, 500 ng/ml hydrocortisone, and 10% FBS.

Human medulloblastoma cell lines, DAOY HTB-186 (DAOY) and D283 Med HTB-185 (DAOY) were routinely maintained in complete growth medium Eagle's Minimum Essential Medium supplemented with 10% FBS with 2 mM glutamine and 100 U penicillin/0.1 mg/mL streptomycin.



UNIONE EUROPEA
Fondo Sociale Europeo



2.2. Plant material

Two *Vitis vinifera* cultivars were used in this study: Aglianico del Taburno, and Falanghina del Beneventano. Berries were collected from a nine-year-old vineyard (145 m a.s.l., Castelvenere, Benevento Province, Southern Italy) during the 2015 growing season. The whole berries were frozen immediately in liquid nitrogen. Three independent pools (biological replicates) of about 100 berries were used for the analyses.

2.3. Extract preparation

To obtain peel and seed semipolar extracts from Aglianico and Falanghina, each tissue was first isolated, minced with liquid nitrogen and then lyophilized. The powder was homogenized with methanol/chloroform (1:4) using TissueLyser (Qiagen). Aqueous phases was then recovered after a 5' centrifugation (12,000 rpm) and lyophilized again. The powder was then dissolved in DMSO (Sigma) at a concentration of 500 mg/ml and stored at -20° C. The extracts were designed as follows: Aglianico grape peel, AGP; Aglianico grape seed, AGS; Falanghina grape peel, FGP; Falanghina grape seed, FGS.

2.4. Cell proliferation assay

To evaluate the effects of peel and seed semipolar extracts from Aglianico and Falanghina on cell proliferation, approximately 1×10^4 cells were plated in 48-well plates and treated with different concentrations of either peel (up to 1000 μ g/ml) or seed (up to 500 μ g/ml) extracts for 24, 48 or 24+24h (24+24). In the case of the 24+24 treatment, cells were treated twice: after



UNIONE EUROPEA
Fondo Sociale Europeo



overnight incubation and again after 24 h. Then, cells were fixed with 3.7% formaldehyde for 10min, washed with PBS, and stained with 0.5% crystal violet for 10 min. A microplate reader (Cytation3, ASHI) was then used to measure the absorbance of each well at 595 nm. All the experiments were performed in triplicate. Through these experiments, we selected the optimal concentration (350 µg/ml) and extract source (seed) to be used in subsequent experiments.

2.5. Colony forming assay

For colony assay, cells were seeded in six-well plates at a density of 500 cells/well and incubated at 37°C in a 5% CO₂ humidified incubator. The culture medium was replaced every three days and cells were grown for 14days. Then, cells were treated with 350µg/ml of Falanghina (FGS) or Aglianico (AGS) seed extracts for 24 h and grown for additional 14 days using media without seed extracts. Colonies were finally stained with crystal violet and counted. Representative plates were photographed using phase contrast microscope (Leica, Milan, Italy). All the experiments were performed in triplicate.

2.6. Wound healing assays

Approximately 1.5×10^5 cells were plated in six-well plates. After overnight incubation, cells were treated with 350 µg/ml of FGS or AGS extracts for 24, 48 and 24 + 24 h. Wounds were created in confluent cells using a 200 µL pipette tip. To analyse cell migration, at least 10 representative images for each scratch were taken in different scratched area of cells at different time



UNIONE EUROPEA
Fondo Sociale Europeo



points of incubation. Images were focused on the centre of the wound field, photographed and measured using ImageJ software. The influence of FGS and AGS on wound closure was compared to scratched cells at time zero hours. All the experiments were performed in triplicate.

2.7. Apoptosis detection by flow cytometry analysis

Approximately 7.5×10^5 cells were plated in 100 mm plates. After overnight incubation, cells were treated with 350 $\mu\text{g/ml}$ of FGS or AGS extracts for either 24, 48 or 24 + 24 h and stained with propidium iodide and annexin V (Annexin V FITC assay, BD Biosciences, Franklin Lakes, NJ), according to the manufacturer's guidelines. Flow cytometry was performed using a FACS-can™ flow cytometry system (Becton Dickinson, San Jose, CA). All the experiments were performed in triplicate.

2.8. RNA extraction and expression analysis of apoptotic pathway genes in MM cells

RNA was extracted using Trizol (Life Technologies) following manufacturer's instructions. For RT-q-PCR assays, 200 ng of total RNA from each sample were retro-transcribed using the High Capacity cDNA Reverse Transcription Kit (Applied Biosystem). RT-q-PCR reactions were performed by means of a 7900 HT Real Time PCR (Applied Biosystem). Gene specific primers for the selected genes: BAX: (Forward 5'-TTTGC TTCAGGGTTTCATCCA-3', Reverse 5'- CTCCATGTTACTGTCCAGTT CGT-3'); (BCL-2: Forward 5'-GTTCCCTTTCCTTCCATCC-3', Reverse 5'-TAGCCAGTCCAGAGGTGAG-3'); FAS: (Forward 5'-CCCTCCTACCT-



UNIONE EUROPEA
Fondo Sociale Europeo



CTGGTTCTTACG-3', Reverse 5'TCAGTCACTTGGGCATTAACACTT-T-3'); FASL: (Forward 5'-CCTGAAAAAAGGAGCTGAGGAA-3', Reverse 5'-GGCATGGACCTTGAGTTGGA-3'); GAPDH: (Forward 5'-CAAGGCTGTGGGCAAGGT-3', Reverse 5'-GGAAGGCCATGCCAGTGA-3'); MDM2 (Forward: 5'-AAGGTGGGAGTGATCAAAGGA-3'; Reverse: 5'-TAGAAACCAAATGTGAAGATGAAGGT-3'); JUN (Forward: 5'-TTTTGCAAGCCTTTCCTGCG-3', Reverse: 5'-TCTTCTCTGCGTGGCT-CTC-3'); DHCR24 (Forward 5'-GCTGGACTCTCCCCGTGTT-3'; Reverse: 5'-TGCCTGTGCCCATGATCA-3') DHCR7 (Forward: 5'-CGCAGGACTTTAGCCGGT-3', Rev: 5'-TGGCTTTGGGAATGTTGGG-T-3'); HMGCR (Forward: 5'-CCTTCCAGAGCAAGCACATTA-3', Reverse: 5'-TTCCCTTACTTCATCCTGTGAGTT-3'); ACAT2 (Forward: 5'-TGTGGCTCCGGAAG-ATGTG-3, Reverse: 5'-GCCTGCTGCCAAGACATGT-3'); FASN (Forward: 5'-CTGCTGCTGGAAGTCACCTATG-3', Reverse: 5'-CGGAGTGAA-TCTGGGTTGAT-G-3'); FDFT1 (Forward: 5'-GGAAGGTGATGCCCAA-GATG-3', Reverse: 5'-ACTGGTCTGATTGAGATACTTGTAGCA-3'); HMGCS1 (Forward: 5'-TGCTGTCTTCAATG-CTGTAACTG-3', Reverse: 5'-ACCAGGGC-ATACCGTCCAT-3').

Primers were designed at exon-exon junctions using Primer express 2.0 (Applied Biosystems). Target expression level was performed as previously described [36] using GAPDH as housekeeping gene. All the experiments were performed in triplicate.



UNIONE EUROPEA
Fondo Sociale Europeo



2.9. Cytochrome *c* release

To determine the cytochrome *c* release from mitochondria to cytosol, cytosolic fractions were isolated after FGS and AGS extracts treatment. 1×10^6 cells were resuspended in 100 μ L of ice-cold plasma membrane permeabilization buffer (200 μ g/ml digitonin, 80 mM KCl in PBS), and incubate on ice for 5 min. Lysates were centrifuged at 800 X g for 5 min at 4 $^{\circ}$ C, and the supernatants (cytosolic fraction) were then collected. All the experiments were performed in triplicate.

2.10. Western blot

Protein extracts were prepared as previously described [37]. For each lane, 20 μ g of total cell lysates were separated in 4–15% Tris–glycine gels (BioRad) at 100 V. Proteins were then transferred to PVDF membranes, probed with the specific primary antibodies, followed by secondary antibodies conjugated with horseradish peroxidase according manufacturer's indications. Primary antibodies used for Western blot include PARP (Cell Signaling, #9542), BCL-2 (Abcam, ab182858), BAX (Santa Cruz Biotechnology, sc-493) and Cytochrome *c* (Abcam, ab133504), MDM2 (Santa Cruz Biotechnology, sc-965), Phospho-c-Jun (Ser243) (Cell Signaling, #32994), p53 (Cell Signaling, #2524). β -Actin (Cell Signaling, #3700) was used as loading control. All the antibodies were used at working concentration indicated by manufacturers. Protein bands were detected by Clarity western ECL (BioRad) and quantified with ImageJ software. All the experiments were performed in triplicate.



UNIONE EUROPEA
Fondo Sociale Europeo



2.13. Statistical analysis

Analysis to evaluate the difference between control and treatments was performed using Graph Pad Prism 9.0 (GraphPad Software, San Diego, CA, USA). For each experiment, overall significance of the differences among means was evaluated using the One-Way ANOVA, while differences of each treatment with the control was evaluated using the Dunnett's multiple comparison test with Bonferroni post hoc correction.

Statistically significant difference compared to untreated cells are: * $p \leq 0.05$, ** $p \leq 0.01$, *** $p \leq 0.001$, **** $p \leq 0.0001$.

All metabolomics data have been statistically validated using an ANOVA with Tukey's t-test analysis.

2.14. Micro-Array analysis

MSTO-211H (1.5×10^6) were treated with 350 ug/ml of AGS for 24+24 hours then RNA was extracted using Trizol (Life Technologies) and following manufacturer's instructions. Total RNA samples were quantified with a spectrophotometer (NanoDrop 1000, Thermo Fisher Scientific, Waltham, MA, United States).

Expression profiling was performed using 100 ng RNA and the Affymetrix Human Clariom S Assay.

(Affymetrix/Thermo Fisher Scientific), which interrogates over 20000 well-annotated genes. Total RNA was converted in labelled ssDNA and used to hybridize microarray. All the procedures including wash and staining of array were performed following Affymetrix instructions.



UNIONE EUROPEA
Fondo Sociale Europeo



After laser scanning .CEL files from array were used for data analysis. Primary data analysis was performed with the Transcriptome Analysis Console software (Thermofisher version 3.1.0.5) including the Robust Multiarray Average module for normalization.

2.15. Pathway and network analysis by IPA.

The list of differentially expressed genes in the MSTO cell line, containing gene identifiers and corresponding expression values, was uploaded into the IPA software (Qiagen). The “core analysis” function included in the software was used to interpret the differentially expressed data, which included biological processes, canonical pathways, upstream transcriptional regulators, and gene networks.

2.16. Oil preparation

The industrial process for the production of grape seeds oil includes a first phase of mechanical separation of grape seeds from the remaining residues of the wine making process. In 100 kg of grapes, 80% is represented by pulp, 12% skin, 4% seeds and the remaining part by stems, and after wine making process, skin and seeds are combined. After separation the grape seeds are dried, at 1.5 atm, at about 60/70° C for about 2 hours. With this process the percentage of water in grape seeds changes from 50 to 10%. At this point the grape seeds pass into a hopper from which oil and a waste product, called flour, comes out. For 100 grams of grape seeds you get about 17 grams of oil and 83 grams of flour.



UNIONE EUROPEA
Fondo Sociale Europeo



The grape seed oil is dissolved in DMSO to a final concentration of 0.9%. Cells are treated with the oil for 48 hours. 0.9% DMSO is added to the control cells.



Results

3.1. Seed rather than peel extracts determine cancer growth inhibition

First of all, we determined that the vehicle with which the extracts, DMSO, were prepared did not affect the viability of the treated cells.

Treatments of MSTO, NCI and Mes2 cells with hydroalcoholic semi-polar peel extract did not affect MM cell viability, also when used at high concentration (1000 $\mu\text{g/ml}$) (**Fig. 3.1**).

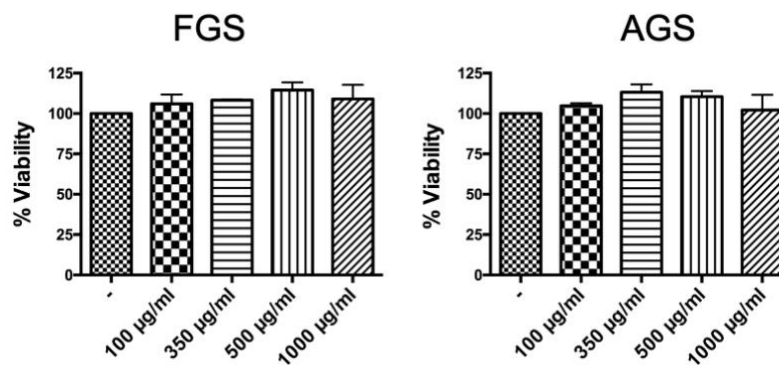


Figure 3.1 Effect of hydroalcoholic semi-polar peel extract on MSTO cells. The same results were obtained with NCI and Mes2 cells. The bars represent the average \pm standard deviation ($n=3$). Statistically significant difference from the control: ** $p<0.01$, *** $p<0.005$, **** $p<0.001$.

On the contrary, extracts from seeds determined cell growth inhibition in a concentration and time-dependent manner (**Fig. 3.2 a, b**). In particular, Falanghina grape seed extract (FGS) at 350 $\mu\text{g/ml}$ was able to significantly decrease MSTO cell viability up to 30% (ANOVA p-value <0.0001). At the



same concentration, Aglianico grape seed extract (AGS) decreased MSTO cell viability up to 40% (ANOVA p-value < 0.0001).

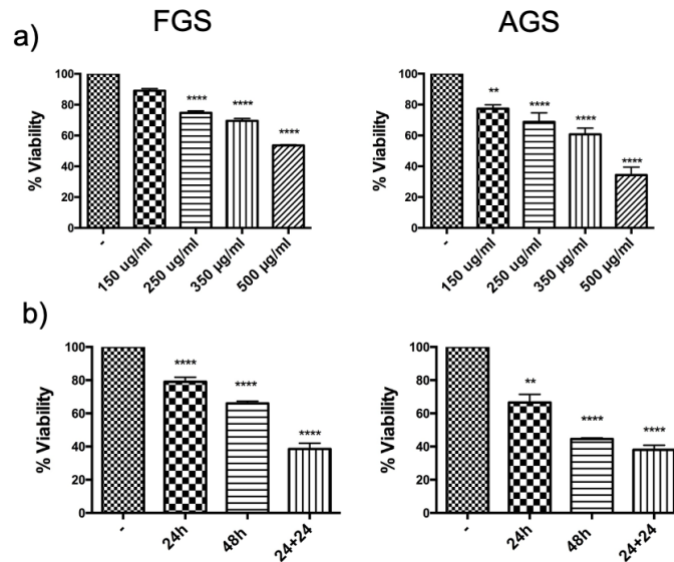


Figure 3.2 Extracts from seeds determined cell growth inhibition in a concentration and time-dependent manner on MSTO cells); untreated cells:-. The bars represent the average \pm standard deviation ($n=3$). Statistically significant difference from the control:

** $p < 0.01$, *** $p < 0.005$, **** $p < 0.001$.

Since AGS at 350 $\mu\text{g/ml}$ resulted closer to the half minimal (50%) inhibitory concentration (IC), we decided to use this concentration for subsequent experiments. Following 48 h of treatment, MSTO cell death was higher than that observed after 24 h. Moreover, a stronger effect was evident when the 48 h treatment was performed by adding the extract twice, every 24 h (24 + 24 h) (ANOVA p-value < 0.0001). (**Fig. 3.2 b**). Similar results were obtained with NCI and Mes2 cell lines (**Fig. 3.3**).

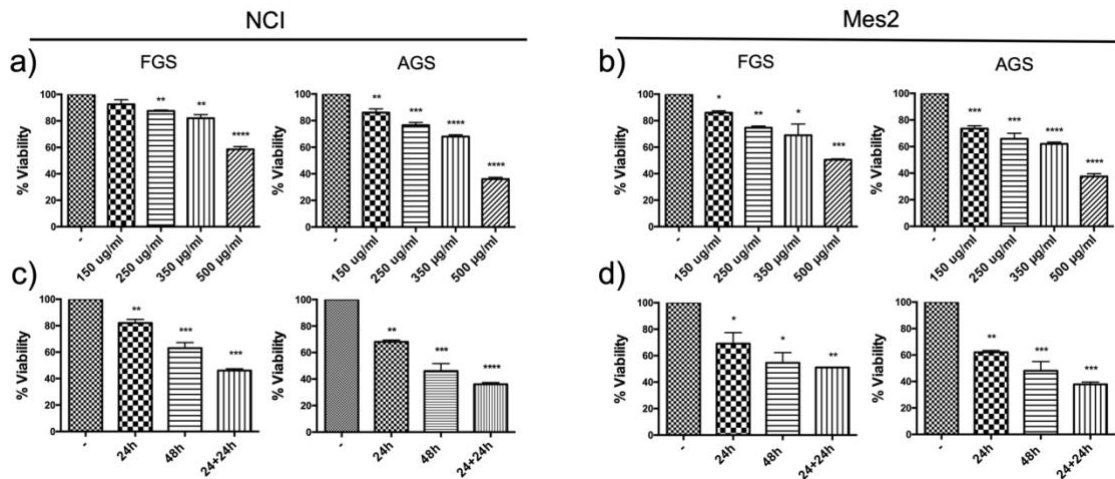


Figure 3.3 NCI and Mes2 cell viability: a, b) treatments with FGS and AGS extracts; c, d) time course treatment with FGS and AGS extracts (350 µg/ml); untreated cells:-.The bars represent the average \pm standard deviation ($n=3$). Statistically significant difference from the control: ** $p < 0.01$, *** $p < 0.005$, **** $p < 0.001$.

These experiments indicated that seed extracts were more effective than peel extracts. For this reason, subsequent assays were carried out only with seed extracts.

3.2. FGS and AGS impair mesothelioma tumorigenic properties affecting cell proliferation and migration

To evaluate the anticancer potential of FGS and AGS, cell migration and invasive ability were analysed on MSTO, NCI and Mes2 treated independently with the seed extracts of Falanghina and Aglianico. The colony formation assay indicates the cellular self-renewal ability and their long-term proliferative potential. Our results showed that this ability was strongly impaired by seed extracts of both varieties in all the cell lines



analysed. In fact, after colonies growth, a 48h treatment with 350 $\mu\text{g/ml}$ of FGS or AGS almost completely inhibited colony formation in MSTO (67% and 90%, respectively; ANOVA p-value < 0.0004) as well as in NCI (51% and 84%, respectively; ANOVA p-value < 0.0001 and in Mes2 cells (48% and 88%, respectively; ANOVA p-value < 0.0003) (**Fig. 3.4**).

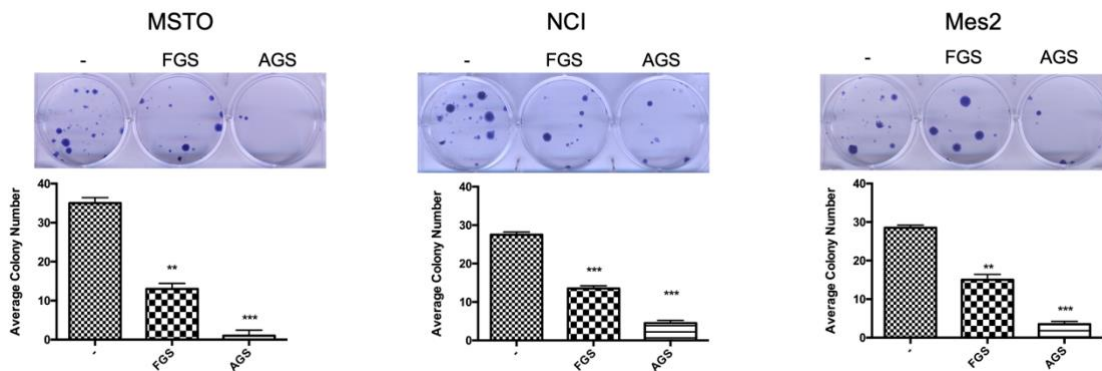


Figure 3.4 Colony formation assay after FGS and AGS treatment (350 $\mu\text{g/ml}$); untreated cells :- . Representative plate images after crystal violet staining are shown. Histograms report average of colony number. The bars represent the average \pm standard deviation ($n=3$). Statistically significant difference from the control: ** $p < 0.01$, *** $p < 0.005$.

To measure the cell migration capability in vitro, we also performed a wound healing assay treating scratched cells with FGS or AGS extracts. MSTO cell migration was significantly inhibited by both extracts in a time-dependent manner reaching a gap of about 120% (FGS; ANOVA p-value < 0.0001) or 170% (AGS; ANOVA p-value < 0.0001) compared to the wound gap in the untreated cells. In particular, the wound gap was maximum after 24 + 24 h treatment with 350 $\mu\text{g/ml}$ FGS or AGS extracts (ANOVA p-value < 0.0001)



UNIONE EUROPEA
Fondo Sociale Europeo



(Fig. 3.5). On the contrary, in the untreated cells the wound gap was closed at the end of the treatment.

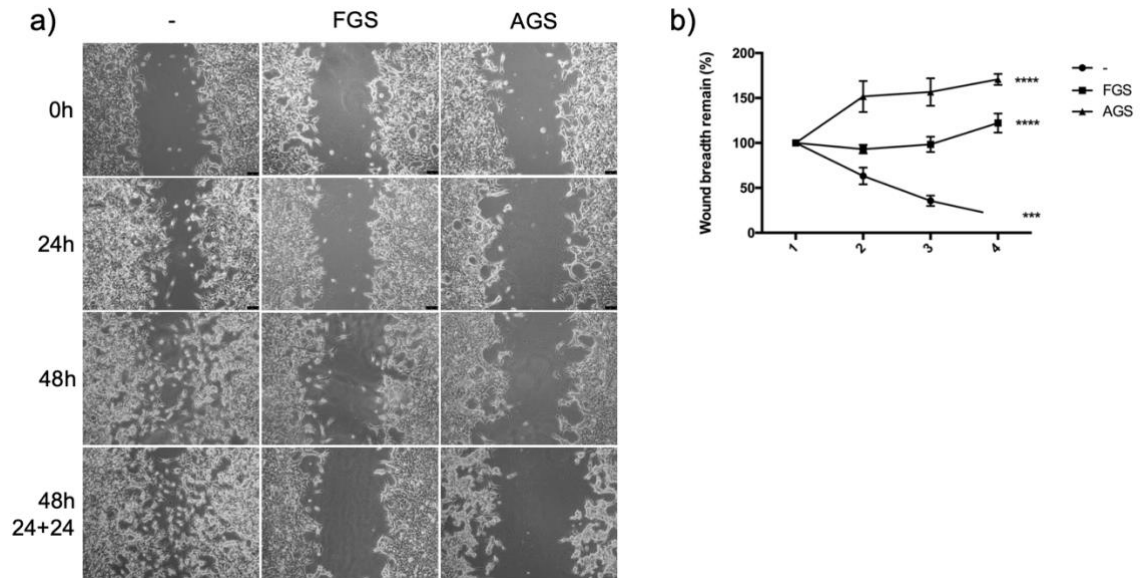


Figure 3.5 Wound healing assay. The wound closure rate was measured by detecting the closure distance at three different time intervals on MSTO cells untreated (-) or treated with 350 $\mu\text{g/ml}$ of seed extracts. Representative micrographs at phase contrast microscope are shown. (h) Quantification of open wound area. The indicators represent the average \pm standard deviation ($n=3$). Statistically significant difference from the control: ** $p<0.01$, *** $p<0.005$, **** $p<0.001$.

Similar results were obtained with NCI and Mes2 cells (Fig. 3.6).



UNIONE EUROPEA
Fondo Sociale Europeo

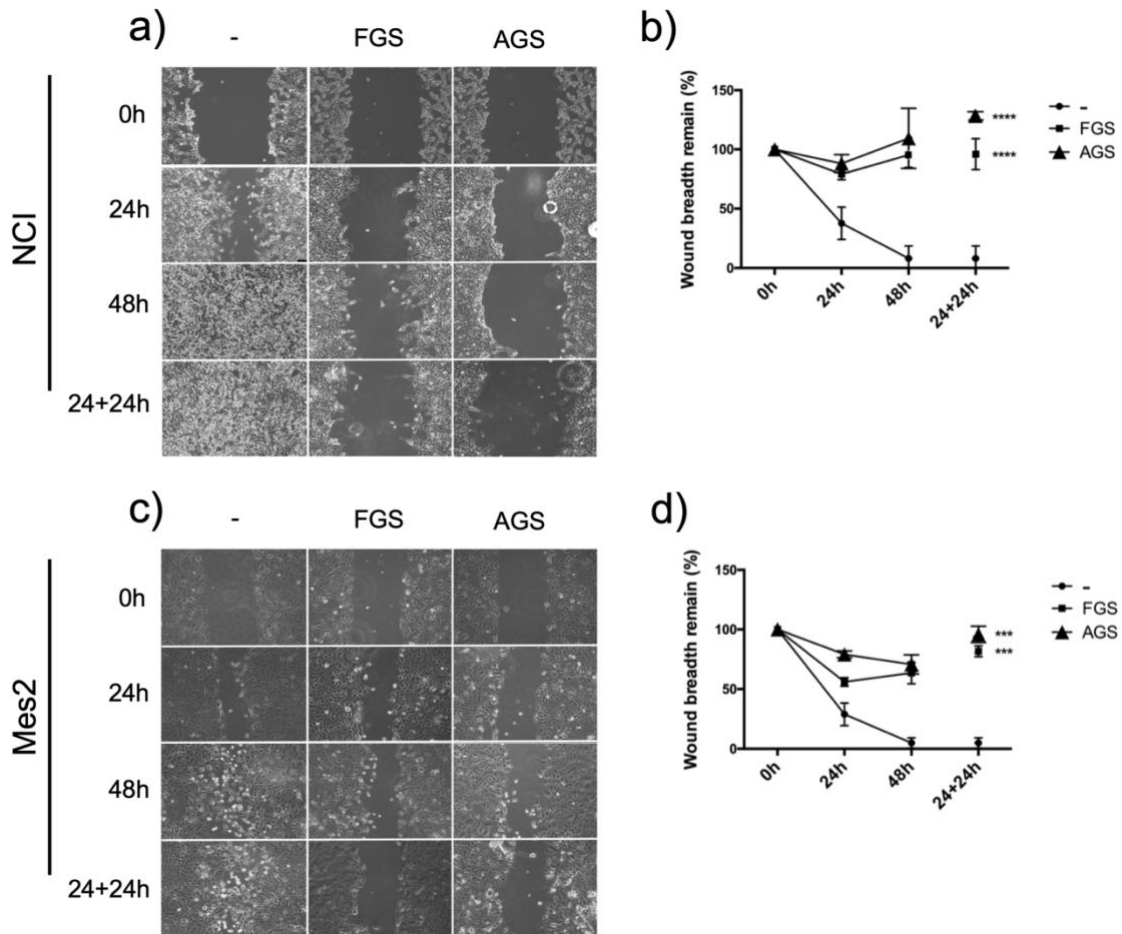


Figure 3.6 Wound healing assay on NCI (a) and Mes2 (c). The wound closure rate was measured by detecting the closure distance at three different time intervals on untreated cells (-) or cells treated with 350 $\mu\text{g/ml}$ of extracts; representative micrographs of the cell migration from three independent experiments are shown. b) and d) Quantification of open wound area. The indicators represent the average \pm standard deviation ($n=3$). Statistically significant difference from the control: *** $p<0.005$, **** $p<0.001$.

Taken together, these results revealed that grape seed extracts from both varieties determined a comparable inhibition in cell growth and migration.



3.3. FGS and AGS induce apoptosis in mesothelioma cell lines

To confirm whether the loss of viability was due to apoptosis, we analysed cell cycle perturbation and the downstream signalling triggered by grape seed extracts. MSTO treatment with FGS determined a growing apoptotic induction during time. It reached about 20% at 24 + 24 h treatment (**Fig. 3.7 a, b**). AGS treatments on MSTO cell lines resulted in apoptotic increase of about 35% after 24 + 24 h treatment (**Fig. 3.7 c, d**) (ANOVA p-value < 0.0051).

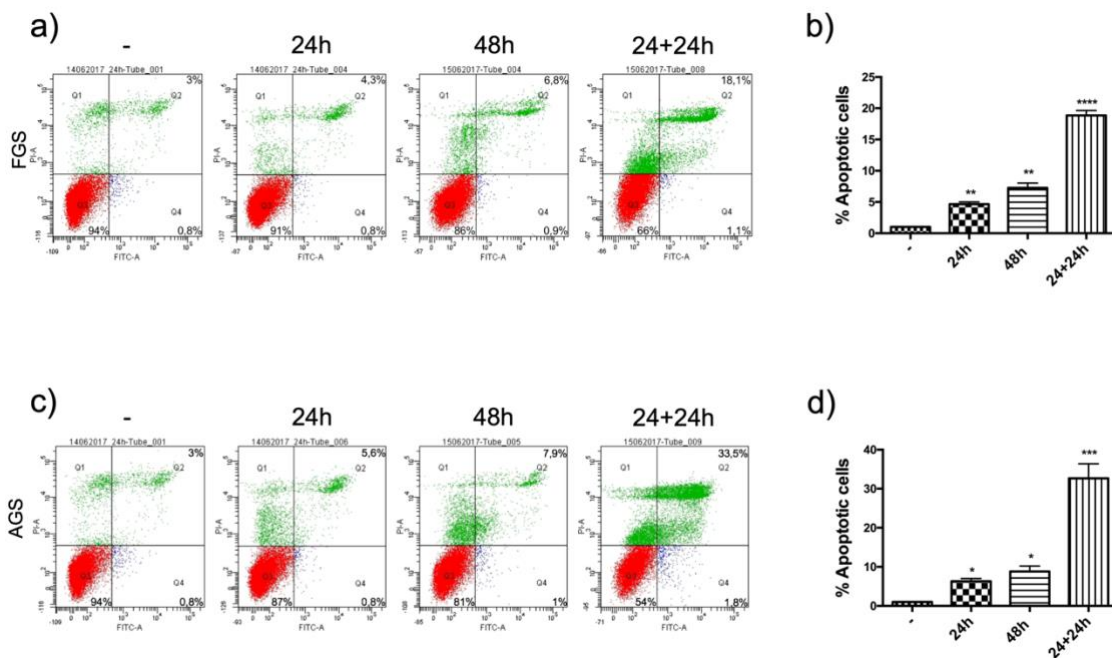


Fig 3.7 MSTO apoptosis analysis by Annexin V-FITC/PI after treatments with 350 $\mu\text{g/ml}$ of FGS (a) and AGS (c) extracts at three different time intervals; untreated cells :- .Q2 and Q4: early and late apoptotic cells; Q1: necrotic fraction; Q3: live cells. Histograms reporting a data summary of the apoptotic index after FGS (b) or AGS (d) treatment represented in (a) and (c). Bars represent the average \pm standard deviation (n=3). Statistically significant difference from the control: * $p < 0.05$, ** $p < 0.01$,

*** $p < 0.005$, **** $p < 0.001$.

The, NCI and Mes2 cell lines showed only slight modifications in apoptosis compared to MSTO. Interestingly, Mes2 cells that did not undergo apoptosis after combined drug treatment with piroxicam and cisplatin [37], resulted more sensitive to both extracts (**Fig. 3.8**), suggesting that grape seed extracts act as broad regulators of apoptotic induction.

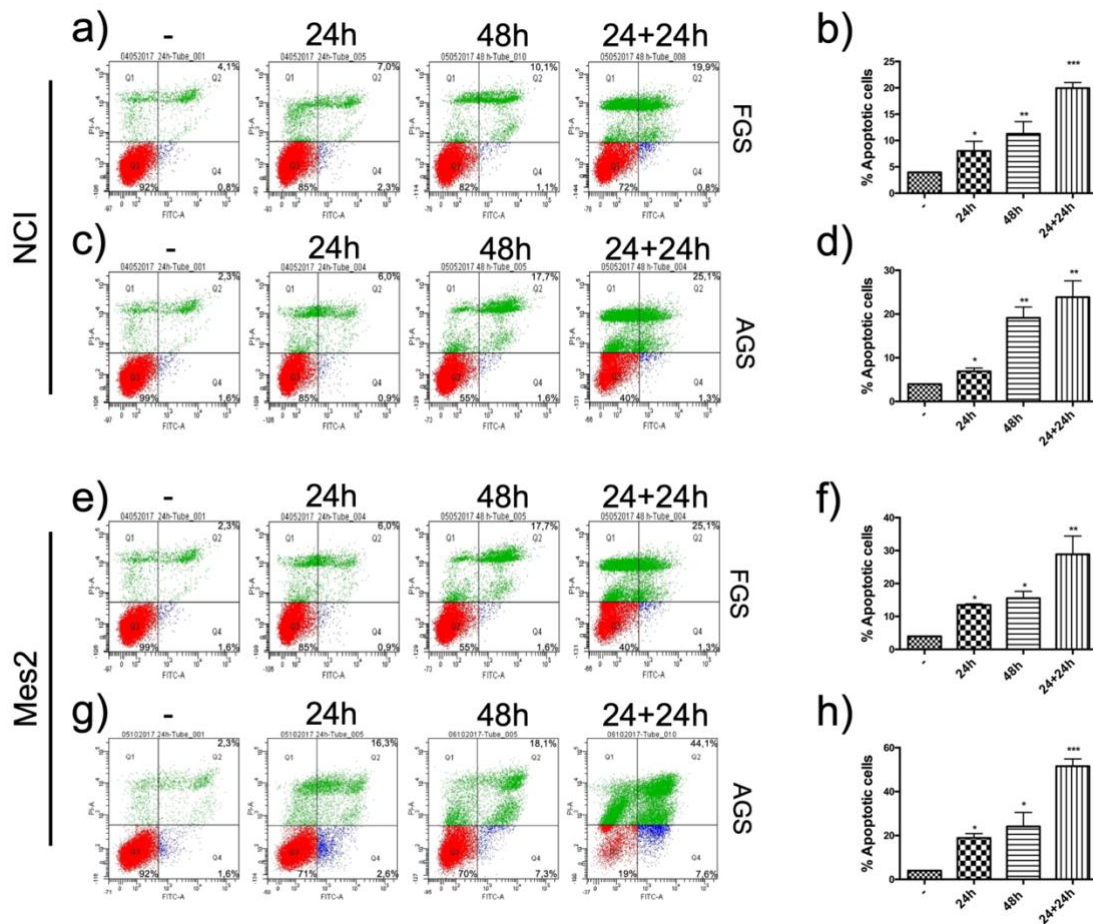


Figure 3.8 NCI (a, c) and Mes2 (e, g) cells were exposed to 350 mg/ml of FGS or AGS for the indicated time and analyzed by flow cytometry analysis (Annexin V-FITC/PI). Histograms reporting a data summary of the apoptotic index for NCI (b, d) or Mes2 (f, h).



h). The bars represent the average \pm standard deviation ($n=3$). Statistically significant difference from the control: * $p<0.05$, ** $p<0.01$, *** $p<0.005$, **** $p<0.001$.

3.4. FGS and AGS activate specific pathways involved in apoptosis

To better investigate the molecular mechanism involved in the apoptotic cell death following FGS and AGS treatments, we focused our attention on the apoptotic pathway involved. We first analysed the expression levels of BCL-2 and BAX after FGS and AGS treatments at 24, 48 and 24 + 24 h by q-PCR. As reported in **Fig. 3.9**, the BAX/BCL-2 ratio suggested a time-dependent apoptotic induction in all MM cell lines analysed. The highest BAX/BCL-2 ratio was observed at 24 + 24 h treatment.

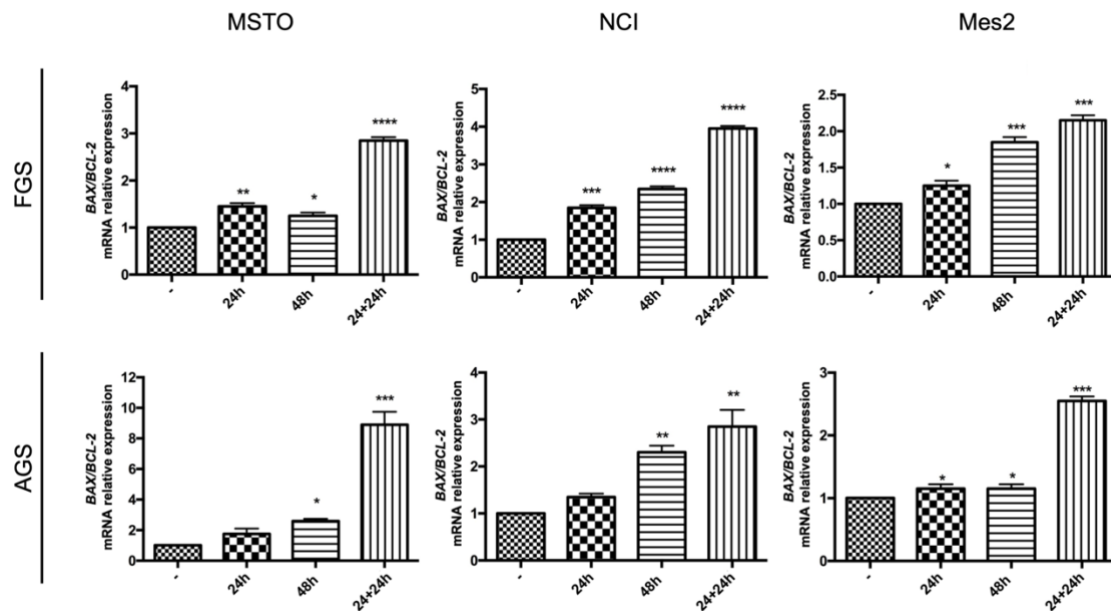


Figure 3.9 Quantitative analysis of mRNA expression levels of Bax and Bcl-2 in MM cell lines. The bars represent the average \pm standard deviation ($n=3$). Statistically significant difference from the control: * $p<0.05$, ** $p<0.01$, *** $p<0.005$, **** $p<0.001$.



UNIONE EUROPEA
Fondo Sociale Europeo



Then, we investigated if grape seed extracts could activate the extrinsic pathway by measuring expression levels of Fas and FasL, two markers of extrinsic apoptosis induction. Our results provided evidence that Fas was not modulated by FGS and AGS in the cell lines analysed. Furthermore, we were not able to detect any expression of FasL (data not shown). These findings indicated that intrinsic but not extrinsic apoptotic pathway is triggered by FGS and AGS treatments.

3.5. FGS and AGS extracts induce protein expression of cleaved PARP and BAX and cytochrome c release

To gain more insight into the molecular mechanism involved in the apoptotic cell death, we also investigated the effect of FGS and AGS extracts on PARP cleavage as well as on BAX and BCL-2 protein expression. PARP protein is very important for cellular function and survival, and it is a well-known caspase enzyme substrate [38]. Immunoblots clearly showed that, in MSTO cell line, both seed extracts induced PARP cleavage and increased ratio of BAX/ BCL-2 (**Fig. 3.10**), confirming that both extracts are able to induce apoptosis.

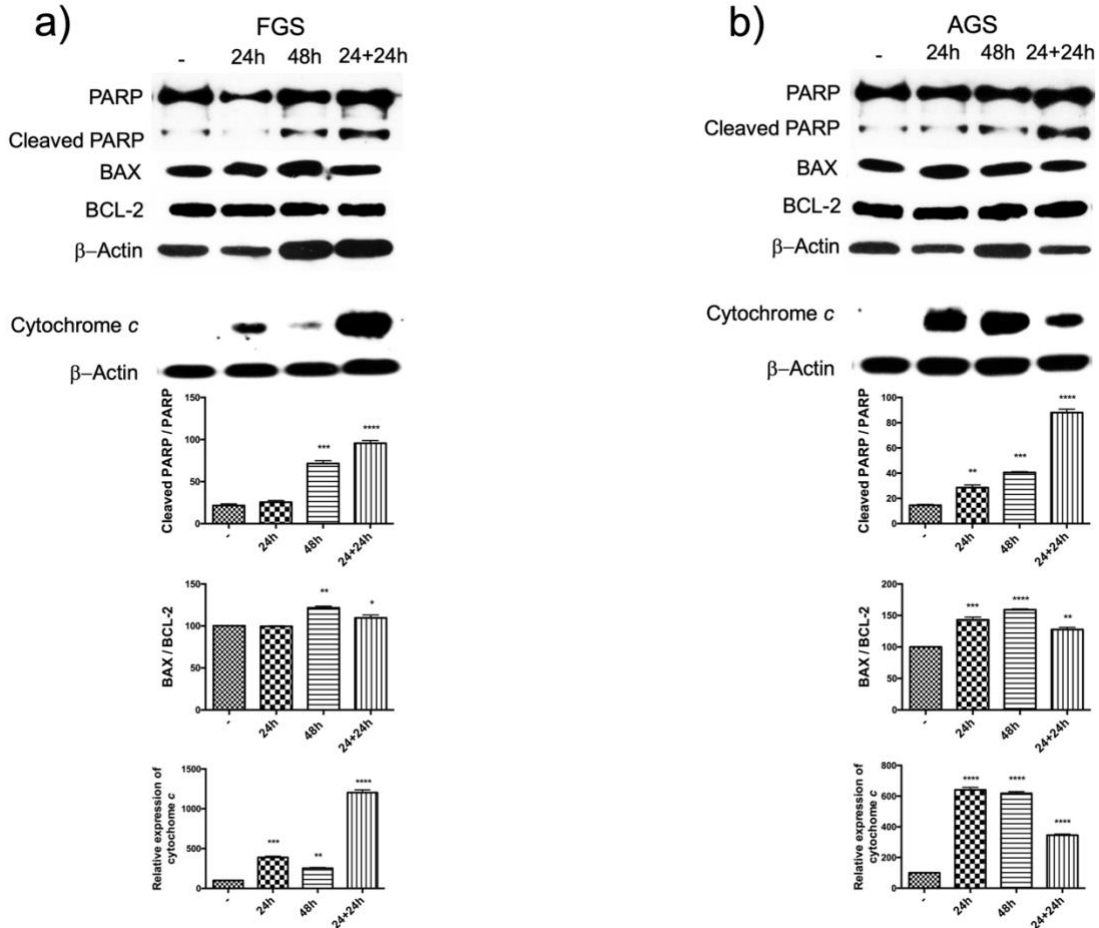


Figure 3.10 Analysis of cleaved PARP, BAX, BCL-2 and of cytochrome c (cytosolic fraction) on MSTO cells treated with FGS (a) or AGS (b) (350 µg/ml); untreated cells: -. β-Actin protein expression was used as loading control. Histograms report the relative expression level. Statistically significant difference from the control: * $p < 0.05$, ** $p < 0.01$, *** $p < 0.005$, **** $p < 0.001$.

Similar results were obtained with NCI and Mes2 cells (**Fig. 3.11**).

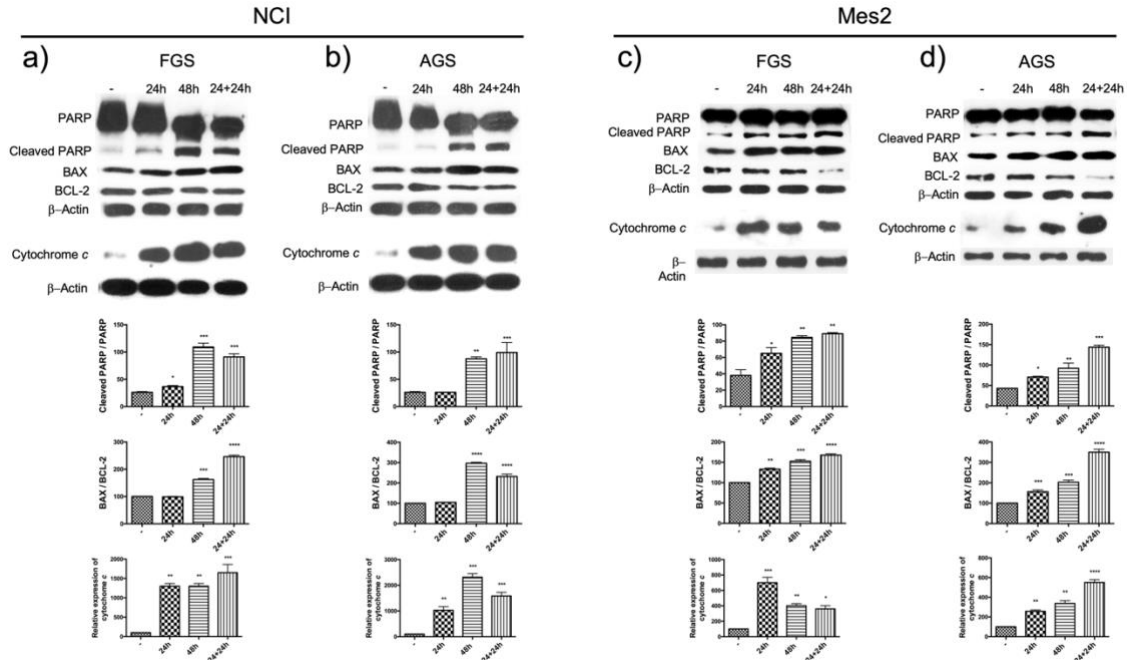


Figure 3.11 Analysis of cleaved PARP, BAX, BCL-2 and of cytochrome *c* (cytosolic fraction) on NCI (a, b) and Mes2 (c, d) cells untreated (-) or treated (350 μ g/ml) with FGS or AGS at three different time intervals. β -Actin protein expression was used as loading control. Histograms report the relative expression level. Statistically significant difference from the control: * $p < 0.05$, ** $p < 0.01$, *** $p < 0.005$, **** $p < 0.001$.

To further investigate the mechanism of grape extracts-mediated apoptosis, we examined the cytochrome *c* release from mitochondria. Indeed, the apoptotic cell death through the intrinsic mitochondrial pathway is known to induce mitochondrial membrane permeabilization and the subsequent cytochrome *c* release. As shown in **Fig 3.10**, treatment with grape seed extracts induced cytochrome *c* release in MSTO cell lines. Similar results were also obtained in NCI and Mes2 cells (**Fig. 3.11**). All these findings, together with earlier observations, suggest that FGS and AGS may directly



UNIONE EUROPEA
Fondo Sociale Europeo



induce mitochondrial membrane damage and, as consequence, cellular apoptosis.

3.6. Metabolomics and transcriptomic analysis of grape peel and seed samples

Cell treatments with seed extracts were very effective, whereas those with peel extracts did not affect cell viability.

To better investigate on the metabolite content of Aglianico and Falanghina seeds a metabolomic analysis and a transcriptomic analysis was performed. Analysis of metabolite content [39] identified a total list of 100 negatively and 241 positively charged ions specifically present or over-/down-represented in seed over peel metabolomes of Aglianico, Falanghina, or in both varieties. The number of compounds that were consistently over- and down-accumulated in seed vs peel tissues was 108 and 154 in Aglianico and 76 and 130 in Falanghina are reported in **Table 1**.

Table 1. Number of statistically significant (p -value ≤ 0.05) over- and down-accumulated metabolites in Aglianico and Falanghina peel and seed extracts.

	AGS/AGP	FGS/FGP	AGS/FGS	AGP/FGP
Over-accumulated	108	76	69	39
Down-accumulated	154	130	123	198

Subsequent analysis indicated that Aglianico and Falanghina seed metabolomes resulted highly enriched in several secondary compounds,



particularly phenylpropanoid precursors and proanthocyanidin. The results can be visualized in the heatmap (**Fig. 3.12**) [39].

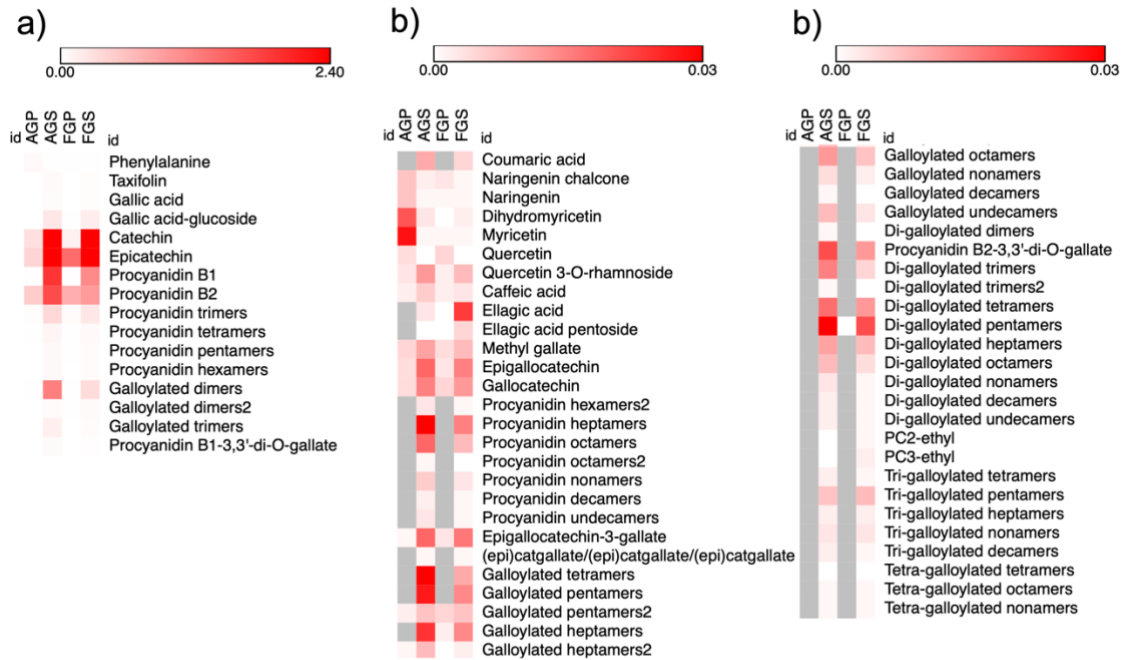


Figure 3.12 Metabolites have been classified in higher- (a) and lower-represented (b), according to the detected values. Red squares of different shades represent the relative values for each metabolite, expressed as fold on the level of the internal standard. Data are present as average \pm standard deviation. Gray squares indicate no detectable expression of the corresponding metabolite.

According to metabolomic analysis gene expression analysis [39] confirmed an increased expression in seeds of genes involved in the phenylpropanoids and flavonoids biosynthesis.



3.7. Microarray analysis

Microarray results allowed to identify the major molecular pathways involved in the response to AGS treatment. Surprisingly, AGS treatment deregulates the cholesterol biosynthesis pathway, and instead, as we expected, it deregulates a pathway involved in apoptosis, which includes the MDM2, JUN, and p53 genes.

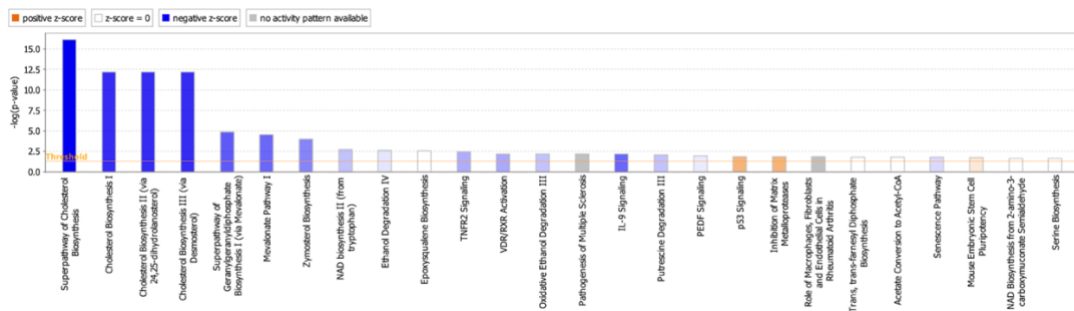


Figure 3.13 Top Canonical Pathway results from IPA

Enriched canonical pathways detected using IPA. A total of 67 enriched canonical pathways were identified by applying the $-\log(P\text{-value})$ are shown in Fig. 3.15. The ‘superpathway of cholesterol biosynthesis’ was the highest ranking signalling pathway with a $-\log(P\text{-value})$ of 2.5. Taking Z-score >2 as the threshold of significant activation.

In addition, the IPA analysis showed that genes deregulated within the class "Diseases and Disorders" are categorized as belonging to cancer, cell death, proliferation and cell viability.

A deeper bioinformatic analysis of cholesterol biosynthesis genes and of those involved in apoptosis, allowed to build a functional network including



a subset of genes in common or having a connection between the two pathways.

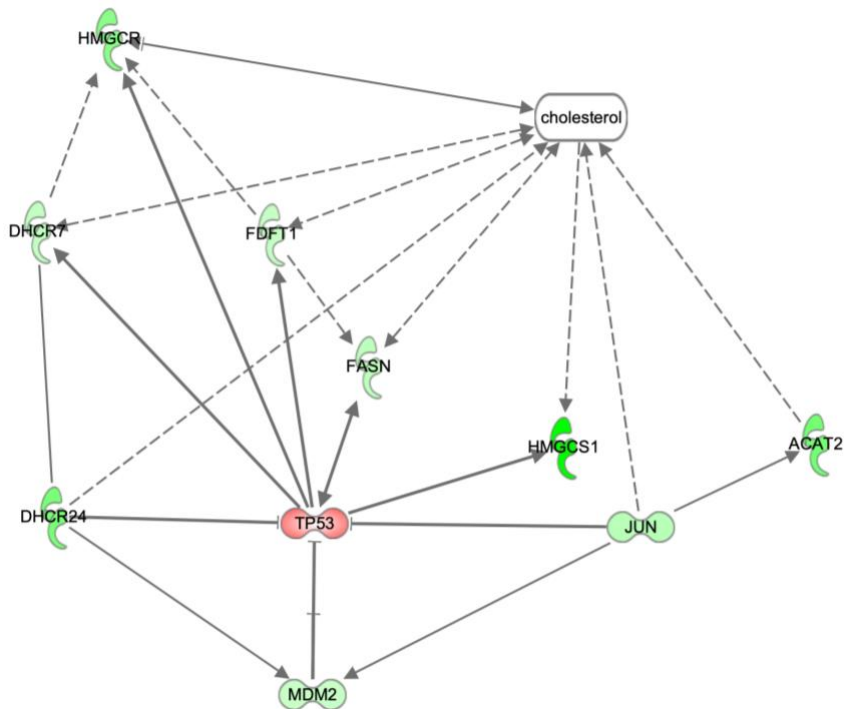


Figure 3.14 *Integrated Network. Biosynthesis and apoptosis pathway genes united in a single network linking them together.*

Specifically, the cholesterol biosynthesis genes chosen were: DHCR24, DHCR7, HMGCR1, ACAT2, FDFT1, HMGCS1, and FASN. All these genes encode proteins involved in the long pathway leading to cholesterol or fatty acid biosynthesis.

DHCR24 and DHCR7, encode for enzymes involved in the last stages of cholesterol formation. DHCR24 is also capable to reduce the activity of p53, directly by reducing its activation, but also indirectly, by increasing the interaction between MDM2 and p53, thus leading to the ubiquitination of the latter.



The expression of these genes connecting the two signalling pathways was biologically validated in all three mesothelioma cell lines by q-PCR. Gene expression analysis confirmed that is downregulated after the treatment with grape seed extract (**Fig. 3.15**)

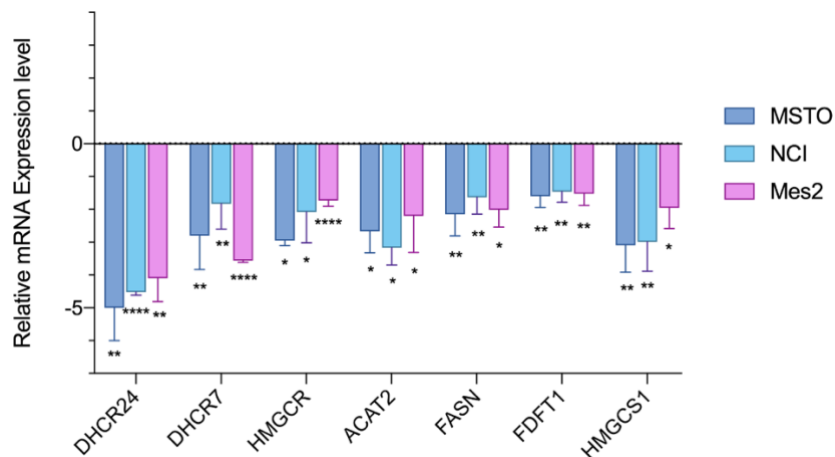


Figure 3.15 Quantitative analysis of mRNA expression levels of genes of cholesterol synthesis in MM cell lines. The bars represent the average \pm standard deviation ($n = 3$).

Statistically significant difference from the control: * $p < 0.05$, ** $p < 0.01$, **** $p < 0.001$.

Among the genes responsible for apoptosis activation, we selected MDM2, JUN and p53. Validation by q-PCR confirmed the results of transcriptomic analysis. In fact, MDM2 and JUN are downregulated, while p53 is upregulated (**Fig. 3.16**)

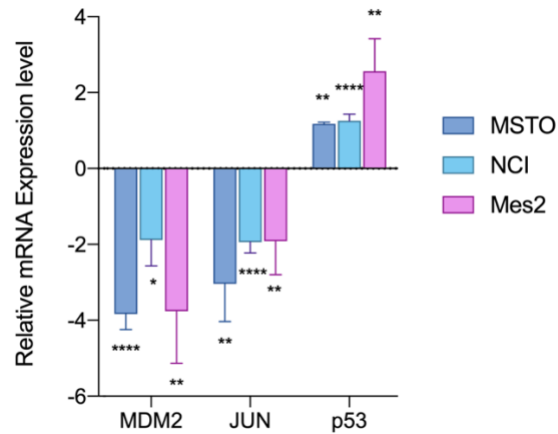


Figure 3.16 Quantitative analysis of mRNA expression levels of genes of apoptotic pathway in MM cell lines. The bars represent the average \pm standard deviation ($n = 3$). Statistically significant difference from the control: * $p < 0.05$, ** $p < 0.01$, **** $p < 0.001$.

The modulation of gene expression found in the MSTO cell line was also confirmed in the other two mesothelioma lines tested, NCI and Mes2.

3.8. AGS and grape seed oil determine growth inhibition in mesothelioma and breast cancer cells.

During the stage carried out in the company, I have studied the grape seed oil production process in order to compare this process with the extraction protocol set up in our laboratory and analysed the resulting product by comparing the biological activity of the oil with the extract.

For this purpose, MSTO cells were treated with 0.9% grape seed oil in DMSO for 48 hours. The results obtained have shown that grape seed oil is capable of reducing the viability of mesothelioma cells, but less than Aglianico extract (**Fig. 3.17**).

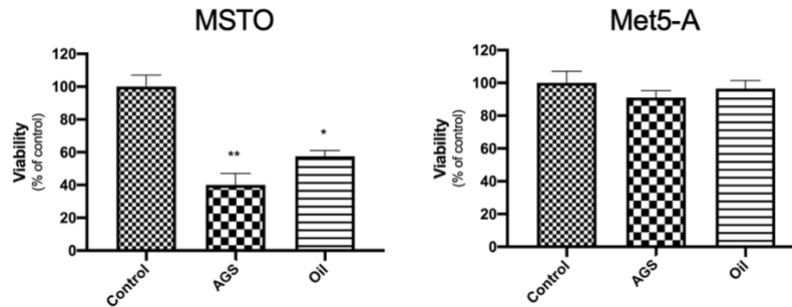


Figure 3.17 Bioactivity of grape seed extracts and grape seed oil on human mesothelioma cells, MSTO, and human mesothelium cells, Met5-A. The bars represent the average \pm standard deviation ($n = 3$). Statistically significant difference from the control: * $p < 0.05$, ** $p < 0.01$.

At this point we tried to understand if the biological activity of Aglianico semipolar extracts and grape seed oil was due to the activation of particular pathways specifically activated in mesothelioma cells or if they could be activated in other tumours as well. Both treatments were therefore initially tested using a breast cancer cell line (MDA-MB-23). In addition, it was verified that the extract had no effect on non-tumour cell counterparts (MCF-10A).

As showed in **Fig. 3.18** both AGS and grape seed oil, are able to reduce cell viability, also in different tumour cell line. However, the treatment with grape seed oil is less effective than AGS treatment in reducing viability.

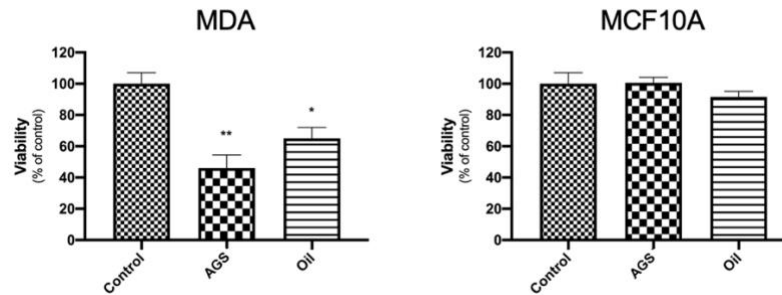


Figure 3.18 Bioactivity of grape seed extracts and grape seed oil on human breast cells, MDA, and mammary epithelial cells, MCF10A. The bars represent the average \pm standard deviation ($n = 3$). Statistically significant difference from the control: * $p < 0.05$, ** $p < 0.01$.

3.9. AGS and grape seed oil bioactivity on mesothelioma and breast cancer cells.

To determine if the reduction in viability was due to apoptosis, we analysed cell cycle perturbation and the downstream signalling triggered by grape seed extracts and grape seed oil. As shown in the **Figure 3.19** MSTO treatment with oil does not determined apoptotic induction, as detected for AGS.

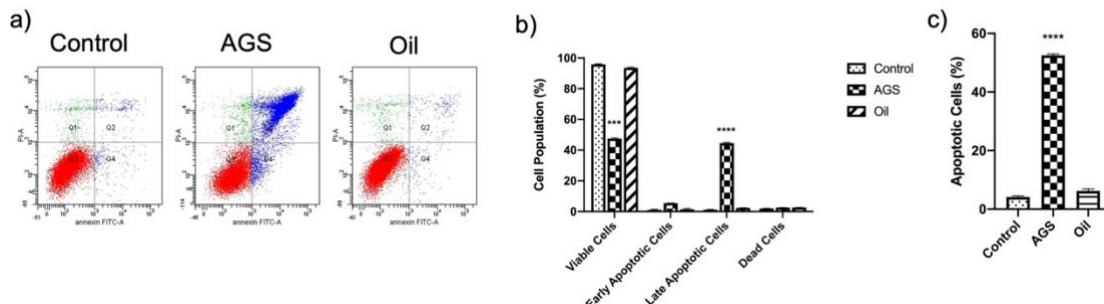


Figure 3.19 MSTO apoptosis analysis by Annexin V-FITC/PI after treatments with AGS or grape seed oil; untreated cells: -.Q2 and Q4: early and late apoptotic cells; Q1:



UNIONE EUROPEA
Fondo Sociale Europeo



*necrotic fraction; Q3: live cells. Histograms reporting a data summary of the cell population (b) and apoptotic index after treatment represented in (c). Bars represent the average \pm standard deviation ($n = 3$). Statistically significant difference from the control: ** $p < 0.01$, *** $p < 0.005$, **** $p < 0.001$.*

Also, in MDA cells treated with AGS the apoptotic process is activated, meanwhile the treatment with the oil does not determine apoptotic induction (Fig. 3.20).

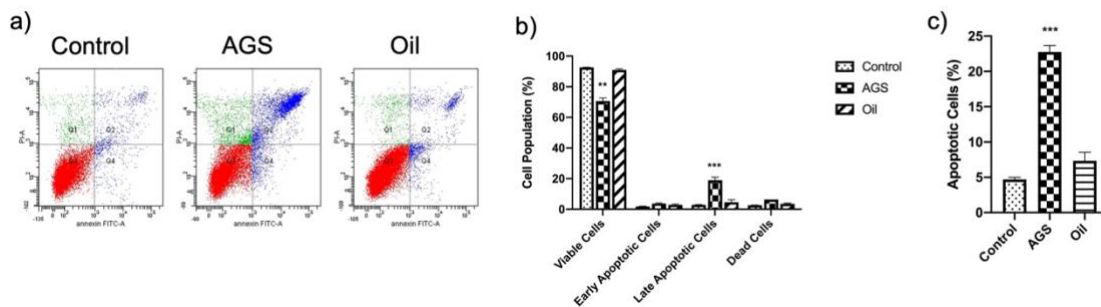


Figure 3.20 MDA apoptosis analysis by Annexin V-FITC/PI after treatments with AGS or grape seed oil; untreated cells:-. Q2 and Q4: early and late apoptotic cells; Q1: necrotic fraction; Q3: live cells. Histograms reporting a data summary of the cell population (b) and apoptotic index after treatment represented in (c). Bars represent the average \pm standard deviation ($n = 3$). Statistically significant difference from the control: *** $p < 0.005$, **** $p < 0.001$.

Therefore, we also compared gene expression of genes after oil treatment and after AGS treatment in MSTO cells. As shown in Fig. 3.21, oil treatment modulates gene expression in the same direction as AGS treatment but with lower efficacy.

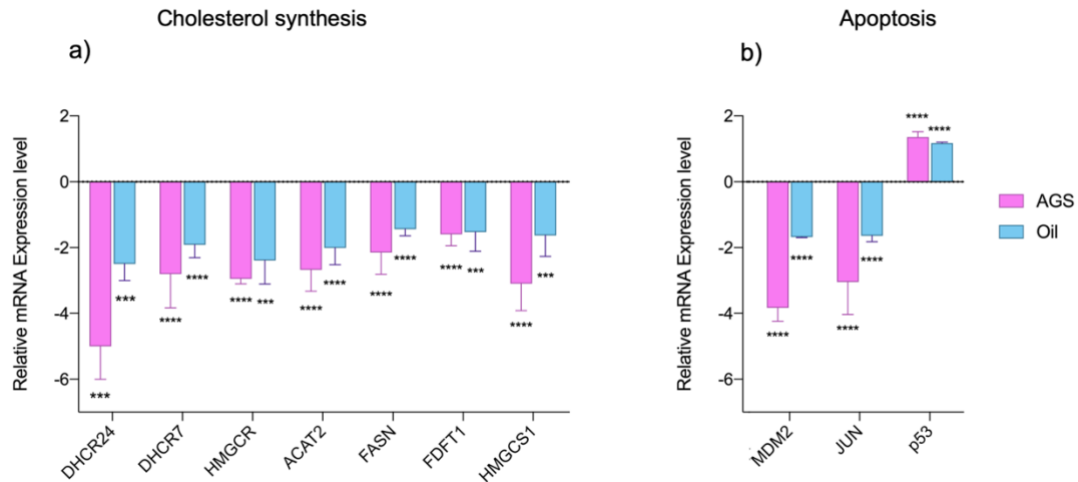


Figure 3.21 Quantitative analysis of mRNA expression levels of genes of cholesterol synthesis and apoptotic pathway in MSTO cell lines. The bars represent the average \pm standard deviation ($n = 3$). Statistically significant difference from the control: *** $p < 0.005$, **** $p < 0.001$.

At this point we analysed the expression of genes present in the integrated network in MDA cells after treatment with AGS or Oil. While the modulation of genes responsible for the apoptotic pathway is the same that we found in mesothelioma cells, in breast cancer cells the cholesterol biosynthesis pathway did not result modulated.

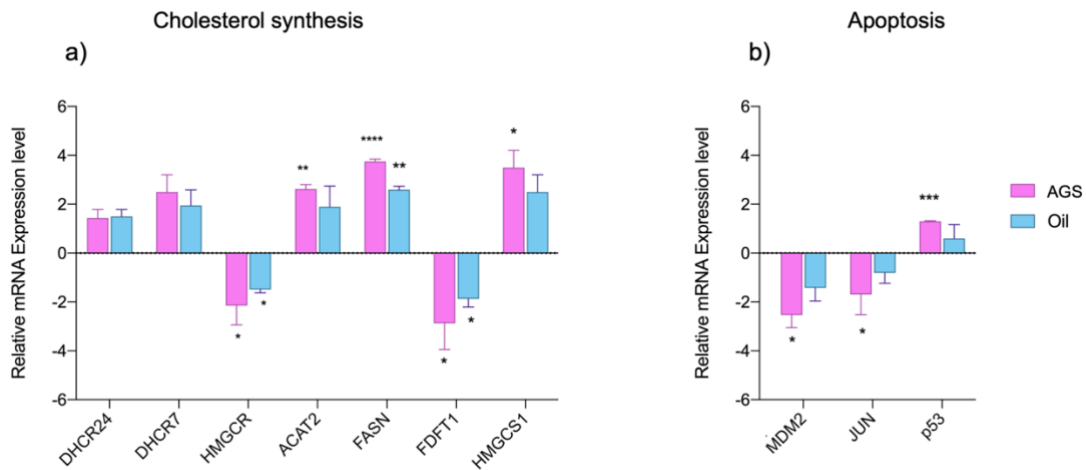


Figure 3.22 *Quantitative analysis of mRNA expression levels of genes of cholesterol synthesis and apoptotic pathway in MSTO cell lines. The bars represent the average \pm standard deviation ($n = 3$). Statistically significant difference from the control: *** $p < 0.005$, **** $p < 0.001$.*

3.10. AGS bioactivity on medulloblastoma cells

To find out if the extract could be also active in other cancers, we have tested the effect of the extract on two medulloblastoma cell lines. The analysis of two cell lines, DAOY and D283, has shown that, also in this case, AGS is able to reduce viability and to induce apoptosis.

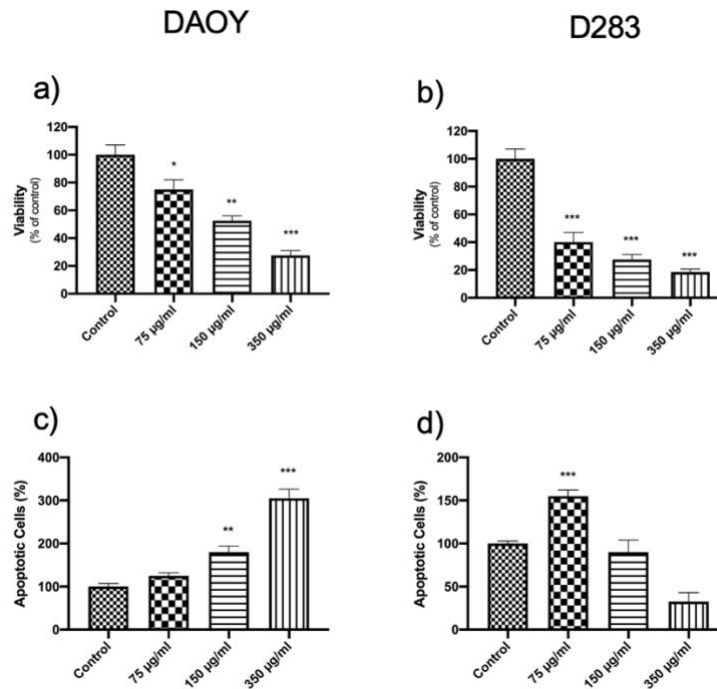


Figure 3.23 Bioactivity of grape seed extracts and grape seed oil on human medulloblastoma cells, DAOY (a) and D283 (b). Apoptotic cells after AGS treatment in DAOY (c) and D283 (d). The bars represent the average \pm standard deviation (n = 3). Statistically significant difference from the control: *p < 0.05, **p < 0.01, ***p < 0.005, ****p < 0.001.

Subsequently, we analysed also in these cells the expression of genes present in the functional network previously identified. The analysis by q-PCR showed that in all cell lines, the genes that regulate apoptosis have the same modulation found in mesothelioma cells. Cholesterol biosynthesis, however, does not seem to be modulated in the same way, in fact, while it is downregulated in DAOY cells, as well as in mesothelioma cells, it does not occur in breast and D283 cancer cells. This allows us to hypothesize that the



inhibition of cholesterol biosynthesis is a pathway specifically activated only in some tumours.

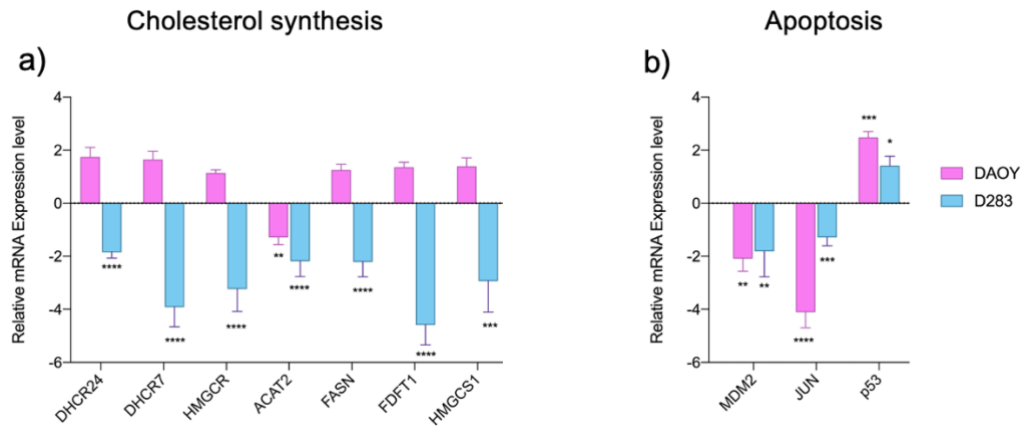


Figure 3.24 Quantitative analysis of mRNA expression levels of genes of cholesterol synthesis and apoptotic pathway in medulloblastoma cell lines. The bars represent the average \pm standard deviation ($n = 3$). Statistically significant difference from the control: * $p < 0.05$, ** $p < 0.01$, *** $p < 0.005$, **** $p < 0.001$.

3.11. Protein expression analysis

Modulation of apoptosis by genes present in the pathway has been confirmed also by protein expression analysis by means of western blot. As shown in **Fig. 3.25** MDM2 protein expression is decreased, as is the expression of phosphorylated c-JUN protein, the active form of c-JUN protein. Furthermore, p53 protein expression was found to be increased in all tumor lines tested.



UNIONE EUROPEA
Fondo Sociale Europeo

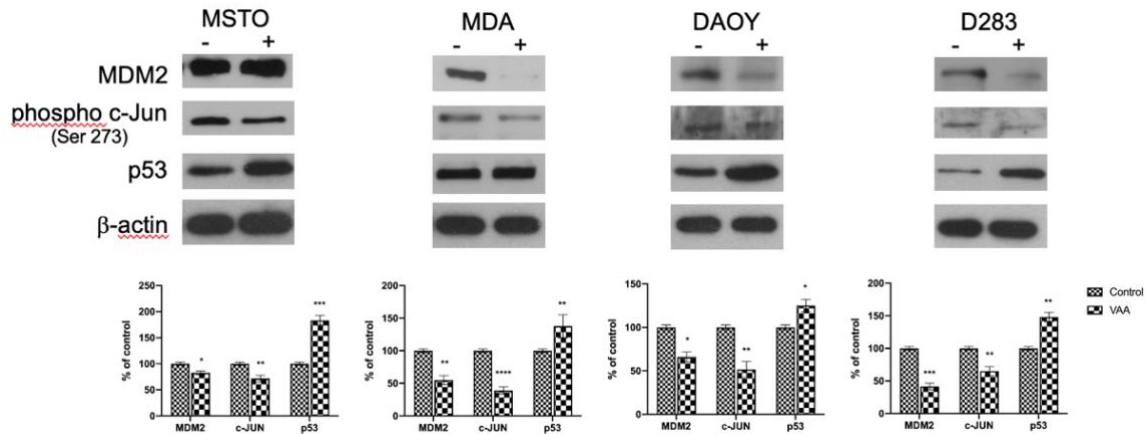


Figure 3.25 Protein expression levels of MDM2, phospho c-JUN and p53 after AGS treatment analysed by Western blot analysis. Histograms report the expression of MDM2, phospho c-JUN and p53 normalized expression. β -Actin was used as loading control. The bars represent the average \pm standard deviation ($n = 3$). Statistically significant difference from the control: * $p < 0.05$, ** $p < 0.01$, *** $p < 0.005$, **** $p < 0.001$.

Finally, the molecular apoptotic pathway activated after AGS treatment in the other tumoral lines was investigated by q-PCR. **Fig. 3.26** indicates that in MDA cells, there is modulation of BAX and BCL2 genes similarly to that found mesothelioma cell lines. Surprisingly, in medulloblastoma cells, BAX and BCL2 genes are not modulated in the same direction, but the expression of death receptor gene FAS, is modulated.

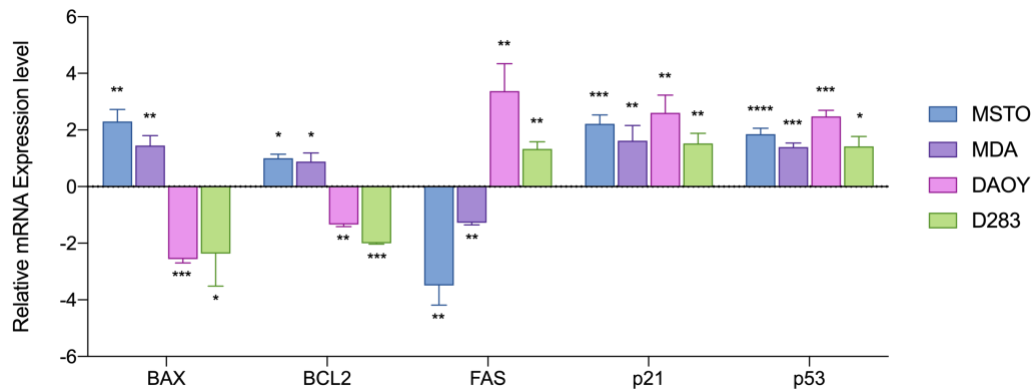


Figure 3.26 Quantitative analysis of mRNA expression levels of Bax, Bcl-2, Fas, p21 and p53 after AGS treatment. The bars represent \pm the average \pm SD of independent experiments ($n = 3$). Statistically significant difference compared to untreated cells: * $p < 0.05$, ** $p < 0.01$, *** $p < 0.005$, **** $p < 0.001$.



UNIONE EUROPEA
Fondo Sociale Europeo



Discussion

The development of alternative and more effective therapies in malignant mesothelioma is deemed urgent since to date the standard therapeutic modalities, including chemotherapy, surgery and radiotherapy have yielded un-satisfactory outcomes. The main objective of our research was to evaluate the anticancer efficacy of semi-polar extracts from peel and seed tissues of two Italian grape varieties, Aglianico and Falanghina, and to determine the mechanisms of action using different human mesothelioma cell lines. Our results suggest that Aglianico and Falanghina peel extracts do not exert proapoptotic effects on MM cells. This agrees with previous studies reporting only chemopreventive or adjuvant effect of peel extracts, mainly for the presence of resveratrol [40]. Additional studies are needed to validate if our peel extracts could act as adjuvant on MM cells when combined to chemotherapeutics. Our data also point out seeds as potential source of phytochemicals with anticancer activities in MM. Indeed, they were able to induce apoptosis in different MM cell lines, including those insensitive to standard chemotherapeutic treatments [37]. Semi-polar seed extracts from both Aglianico (AGS) and Falanghina (FGS) affected tumorigenic properties of human mesothelioma cells in a time- and dose-dependent manner, with Aglianico showing the strongest effect. Colony formation assay showed that FGS and AGS reduced the capacity of mesothelioma cells to form colonies, indicating that these extracts impair cellular self-renewal ability and proliferative cell rate. In addition, as assessed by a wound-healing assay, FGS



UNIONE EUROPEA
Fondo Sociale Europeo



and AGS displayed the capacity to significantly inhibit cell migration capability.

We provided evidence that cell viability reduction after FGS and AGS treatments was due to apoptosis. Indeed, we found that FGS and AGS trigger a time-dependent increase of the BAX/BCL-2 ratio and of cytochrome *c* release in all mesothelioma cell lines analysed, with the highest threshold reached after the 24 + 24 h treatment. BAX and BCL-2 are two members of the BCL family with an opposite role in regulating mitochondrial function and cytochrome *c* release. Alterations of mitochondria homeostasis represent one of the main pathways involved in apoptosis. In non-apoptotic cells, BAX is mainly located in the cytosol, while BCL-2 is found in the mitochondrial membranes. Upon apoptosis induction, BAX translocates into mitochondria triggering permeabilization of mitochondrial outer membrane with cytochrome *c* release. The apoptotic factors are then released into the cytoplasm and transferred to the nucleus, where they induce apoptosis. The pro-survival BCL-2 acts as antiapoptotic protein by preventing mitochondrial outer membrane permeabilization and inhibiting the transfer of apoptosis-inducing factors to the nucleus. BAX/BCL-2 ratio regulates the mitochondrial intrinsic apoptosis pathway with subsequent cytochrome *c* release in the cytoplasm.

Several studies described the anticancer activity of grape seed standardized extracts against different human cancer cell lines such as breast, colon, lung and skin [41] due to the presence of specific metabolites residues (gallate esters, pyrogallol) [42-44]. Our *in vitro* study showed, for the first time, the effectiveness of complex semi-polar extracts from Aglianico and Falanghina



UNIONE EUROPEA
Fondo Sociale Europeo



seeds, suggesting that a specific combination of active compounds characterizes a grape variety and influences its biological activity. Other studies using semipolar fractions extracted from mature red grape seeds showed that they affected cell viability and enhanced Fluorouracil toxicity of 5-FU in Caco-2 cells [44]. Therefore, to gain a first clue about the source of this bioactivity, we exploited high-resolution metabolomics to investigate the composition of the compounds accumulated in the peel and seed extracts of the two grape varieties. Overall, resulted highly enriched in proanthocyanidin molecules, which were present at very low levels or totally undetected in the peel samples of both varieties. Interestingly, Aglianico seeds displayed higher total proanthocyanidins. This finding agrees with the stronger inhibitory effect of Aglianico compared to Falanghina seeds on MM cell lines. Transcriptional data confirmed these results indicating that proanthocyanidins represent the main class of compounds accumulated in seed extracts.

With respect to the detected bioactivity of AGS and FGS extracts, metabolomics data suggest that phenylpropanoids, particularly proanthocyanidins, are responsible or at least greatly contribute to the anticancer activity; in this context, we cannot exclude that additional compounds may take part in this process, and future fractionation studies will be carried out to unravel the molecules whose accumulation is mostly associated to the bioactivity.

This is the first study indicating that grape seed semi-polar extracts are effective in MM cells. Moreover, studies on the molecular mechanisms identified that apoptotic intrinsic signalling pathways is involved. Our



UNIONE EUROPEA
Fondo Sociale Europeo



findings will provide the reference for future analyses to identify the metabolic fraction/s mainly responsible/s for this bioactivity, thus to produce more effective extracts; in addition, this study will allow planning more detailed *in vivo* experiments relevant to the treatment of MM and possibly for clinical applications.

Analysis of transcriptomic pathways showed that the main pathways involved by AGS treatment were those of cholesterol biosynthesis. This result was extremely surprising, while we expected a major involvement of pathways related to the cell death of cancer cells. Cholesterol plays a fundamental role in the cellular structure, in fact it is an indispensable component of the cellular membrane, so its deficiency can cause serious dysfunction in the cells. p53 protein plays a key role in controlling the initiation and development of cancer by regulating cell cycle arrest, apoptosis, senescence, and DNA repair. MDM2 protein is a major negative regulator of p53 that inhibits the activity of p53 and decreases its protein stability [45]. The dysregulation of the p53-MDM2 pathway, involving p53 mutations or deletions and/or MDM2 amplification and overexpression, is the most commonly observed molecular modification in various human cancers [46-48]. c-JUN, the protein encoded by the JUN gene, blocks p53 activity, its over expression represses p53 expression and accelerates cell proliferation [49]. The connection between the two pathways is represented by the DHCR24 gene. This gene encodes for an enzyme involved in the long chain of cholesterol synthesis. This enzyme, 24-Dehydrocholesterol reductase catalyses the reduction of the delta-24 double bond of sterol intermediates during the final steps of cholesterol biosynthesis. Therefore, a



UNIONE EUROPEA
Fondo Sociale Europeo



reduced expression of DHCR24 induces a consequent reduction of cholesterol synthesis [50]. On the other hand, the same DHCR24 protein blocks the activity of p53. DHCR24 acts in two different ways, in fact it is able to directly reduce the activation of p53 [51], preventing the acetylation of this protein, that in turn stabilizes and increases the activity of p53.

At the same time DHCR24 is also capable of preventing the binding between p53 and MDM2. This binding promotes the elimination of p53 by ubiquitination. It is reported that overexpression of DHCR24 reduces p53 levels [52]. Thus, in our case, a reduction in DHCR24, MDM2, and JUN leads to an over expression of the onco-suppressor p53, a very common mechanism of action observed in treatment with natural products against cancer [53]. What is very interesting is that the effect of grape seed treatment is the same even in Mes2 mesothelioma cells that are resistant to standard chemotherapy treatment due to the lack of p21.

The extraction protocol from grape seeds developed in the laboratory allowed us to obtain a very small amount of extract. During the period in the company, I was able to study the process of industrial production of another product obtained from grape seeds, grape seed oil, an oil marketed and used in cooking. This allowed me to see what the commonalities were between the laboratory extraction protocol and the industrial process, and how the latter could be adapted to obtain a product as similar as possible to the laboratory extract but on an industrial scale.

Having studied the production process, we investigated the biological effects of grape seed oil on cells and compared with effect of AGS. We have seen that oil is capable of reducing viability in both mesothelioma and breast



UNIONE EUROPEA
Fondo Sociale Europeo



cancer cells, but that unlike AGS this reduction in viability is not due to induction of the apoptotic process.

Modulation of gene expression in the integrated network is also less effective than treatment with AGS. These results could be due to the fact that the oil we used is a commercial product produced from grape seeds of different cultivars, as we have previously seen different cultivars such as Aglianico and Falanghina have different biological effects. Therefore, it would be appropriate for future research to use an oil produced only from Aglianico seeds.

Results obtained with medulloblastoma cells have confirmed that treatment with AGS reduces viability and induces apoptosis also in other tumour types, leading us to suppose that the mechanism of action is also valid for other tumour types and not linked to some typical feature of a single tumour type. This assumption has been validated by modulation of gene expression of the apoptosis pathway in medulloblastoma cells. In fact, while the cholesterol synthesis pathway is only modulated in certain tumour types, the pathway leading to p53 activation is conserved in all cell lines tested. Further confirmation is the modulation of protein expression level in all the lines analysed, where there is a reduction in p53 inhibitors, MDM2 and JUN, and an increase in p53 itself.

The expression of BAX, BCL2 and FAS genes in the different cell lines highlights even more the central role of p53. In fact, if the apoptotic process is triggered by different pathways in different cells, all of them converge in the activation of p53.



UNIONE EUROPEA
Fondo Sociale Europeo



Chapter 2

Polyphenols from Ginkgo biloba extract



UNIONE EUROPEA
Fondo Sociale Europeo



Materials and methods

4.1. Cell Culture and Chemicals

Human neuroblastoma cell line, SK-N-BE(2) (CRL-2271, ATCC®, LGC Standards S.r.l., Milan Italy) were cultured at 37 °C in a 5% CO₂ humidified incubator in either RPMI-1640 medium (Euroclone spa, 20016 Pero, MI) supplemented with 10% fetal bovine serum (FBS), glutamine (2 mM), sodium pyruvate and antibiotics (0.02 mg/mL streptomycin and 0.02 IU/mL penicillin).

Ginkgo biloba L. extract EGb 761 (EGb) was a gift from Schwabe (Schwabe Pharma Italia Srl, Egna, Italy). EGb stock solution contained 250 mg/mL of extract was dissolved in dimethyl sulfoxide (DMSO). Hydrogen peroxide (H₂O₂) (Sigma-Aldrich, St. Louis, MI, USA) was used as oxygen stress inducer.

4.2. Cell Proliferation Assay

For each experiment, approximately 1.5×10^5 cells/well in 6-well plates were plated and treated as described and untreated cells were used as control. To identify the H₂O₂ concentration able to determine about 50% of viability decrease, SK-N-BE cells were treated with 25, 50, 75, and 100 mM of H₂O₂ for 24 h. When specified cells were treated with 25 µg/mL EGb for 24 h, the medium was replaced before H₂O₂ treatment.

To evaluate the effect of EGb on cell viability, cells were treated with 10, 25, and 50 µg/mL for 24 h. To estimate the protective effect of EGb cells were treated for 24 h with 25 µg/mL of EGb, then insulted with 75 µM of H₂O₂ for



UNIONE EUROPEA
Fondo Sociale Europeo



additional 24 h. EGb was dissolved in DMSO. Untreated samples were exposed to 0.1% DMSO and were used as control.

For each experiment after treatment cells were collected and counted with Trypan Blue solution. (T6146, Sigma-Aldrich, St. Louis, MI, USA).

All the experiments were performed in triplicate. Data are expressed as the mean \pm SD.

4.3. Propidium Iodide and DAPI Staining Assay

In 6-well plates approximately 1.5×10^5 cells/well were plated and treated with EGb and H₂O₂ as previously described. After treatment cells were stained with 10 mg/mL of Propidium Iodide (PI) (Bioshop, Burlington, ON L7L 6A4, Canada) and DAPI (4',6-diamidine-2'-phenyl indole dihydrochloride, Roche, Mannheim, Germany). Representative images were taken using fluorescent microscope (DMI8, Leica, Instruments, Germany) and fluorescence was quantified using Leica Application Suite X software (Leica, Milan, Italy). All the experiments were performed in triplicate. Data are expressed as the mean \pm SD.

4.4. Mitochondria Membrane Potential Measurement

Mitochondria membrane potentials (MMP) were measured by JC-10 (Sigma-Aldrich, St. Louis, MI, USA) following the manufacturer's instructions. Loss of MMP was indicated by a progressive JC-10 dislocation from mitochondria to the cytosol. Cells were photographed using fluorescent microscope (DMI8, Leica, Instruments, Germany). Red (540/570 nm) and green (485/534 nm) fluorescence was quantified by Leica Application Suite X (LAS



UNIONE EUROPEA
Fondo Sociale Europeo



X) (Leica, Milan, Italy). All the experiments were performed in triplicate. Data are expressed as the mean \pm SD.

4.5. RNA Extraction and q-PCR

RNA extraction and q-PCR were essentially performed as previously described. Briefly, Total RNA was isolated from each sample with Trizol (Thermo Fisher Scientific, Waltham, MA USA), as indicated by manufacturer. For each sample to analyse, cDNA was then obtained starting from 200 ng of total RNA using High Capacity cDNA Reverse Transcription Kit (Applied Biosystem, Thermo Fisher Scientific, Waltham, MA USA). The described selected genes using gene specific primers BAX: Forward 5'-TTTGCTTCAGGGTTTCATCCA-3': Reverse 5'-CTCCATGTT-ACTGTCCAGTTCGT-3'; BCL- 2: Forward 5'-GTTCCCTTTC-CTTCCATCC-3'; Reverse 5'-TAGCCAGTCCAGAGGTGAG-3'; p53: Forward 5'-TCTGTCCCTTCCCAGAAAACC-3'; Reverse 5'-CAAGAA-GCCCAGACGGAAAC-3'; GAPDH: Forward 5'-CAAGGCT-GTGGGC-AAGGT-3'; Reverse 5'-GGAA GGCCATGCCAGTGA-3'.

All primers were selected using a specific software (Primer express 2.0, Applied Biosystems, Foster city, CA, USA) and all of them specifically covered the exon-exon junctions. The analysis of gene expression was done as described in [37] and GAPDH gene was used as internal control. q-PCRs were done using the 7900 HT Real Time PCR (Applied Biosystem) and for each experimental condition a triplicate was performed. Data obtained are expressed as the mean \pm SD.



UNIONE EUROPEA
Fondo Sociale Europeo



4.6. Western Blot

For each experimental condition and from each sample total, protein extracts were obtained, as described in [54]. For the analysis, 20 μg of each sample were loaded on Tris–glycine gradient gels (4% to 15% gels (Bio-Rad Laboratories, Inc., Hercules, CA, USA) and separated at 100 V. To probe proteins with specific primary antibodies antibodies, they were transferred to PVDF membranes (Biorad Laboratories, Inc., Hercules, CA, USA). All the secondary antibodies used were horseradish peroxidase conjugated. All the antibodies were used as indicated by manufacturer. The following primary antibodies were used for Western blot: PARP (Cell Signaling, #9542), BCL-2 (Abcam, ab182858), BAX (Santa Cruz Biotechnology, sc-493), Acetyl-p53 Lys382 (Cell Signaling, #9542). As the internal control we used β -Actin (Cell Signaling, #3700), which was used as the loading control. To detect protein levels, Clarity western ECL (Bio-Rad Laboratories, Inc., Hercules, CA, USA) was used. The quantization was then obtained using ImageJ software vJ1, an open source tool. For each experimental condition a triplicate was performed, and results are expressed as the mean \pm SD.

4.7. Statistical Analysis

To perform calculations on sample size the on line available software GPower was used. Sample size was determined using as parameters: $1 - \beta = 0.80$, $\alpha = 5\%$. For each experiment, statistical analysis was done using Graph Pad Prism 9.0 (GraphPad Software, San Diego, CA, USA) to analyse the significance of the differences between control and treatments. We evaluated the differences among means applying the one-way ANOVA. Bonferroni's



UNIONE EUROPEA
Fondo Sociale Europeo



multiple comparison test with Bonferroni post hoc correction was used to analyse the differences of each treatment respect to the control.

Statistically significant difference compared to DMSO treated cells are: * $p \leq 0.05$, ** $p \leq 0.01$, *** $p \leq 0.001$, **** $p \leq 0.0001$.



Results

5.1. EGb Protects SK-N-BE Cells Against Oxidative Stress Induced Apoptotic Cell Death

We first determined, in a dose-response curve at 24 h, the amount of H₂O₂ that had lethal effect on SK-N-BE human neuroblastoma cells. Oxidative stress induced cell death was around 50% when cells were treated with 75 μM H₂O₂ (Fig 5.1).

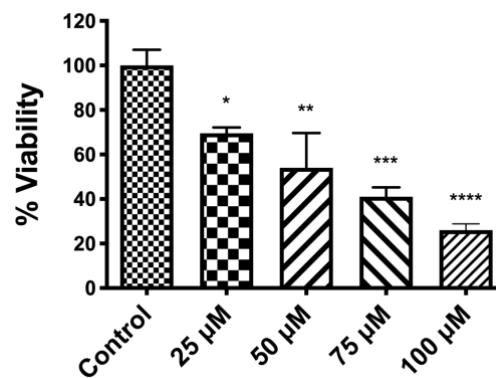


Figure 5.1 H₂O₂ affects SK-N-BE cell viability. Cell viability decrease after treatments with different concentration of H₂O₂. The bars represent \pm the average \pm SD of independent experiments ($n = 3$). Statistically significant difference compared to control cells: * $p \leq 0.05$, ** $p \leq 0.01$, *** $p \leq 0.001$, **** $p \leq 0.0001$.

To verify if 75 μM H₂O₂ was able to induce apoptosis on SK-N-BE cells, untreated and H₂O₂ treated cells, without fixation and permeabilization, were stained with Annexin V - FITC and PI. The analysis by fluorescence microscopy confirmed that H₂O₂, at this concentration, induced apoptosis



UNIONE EUROPEA
Fondo Sociale Europeo



(**Fig 5.2 a**). Indeed, a strong increased number of stained Annexin V - FITC and PI cells were present when cells were treated with H_2O_2 (**Fig. 5.2 b**).

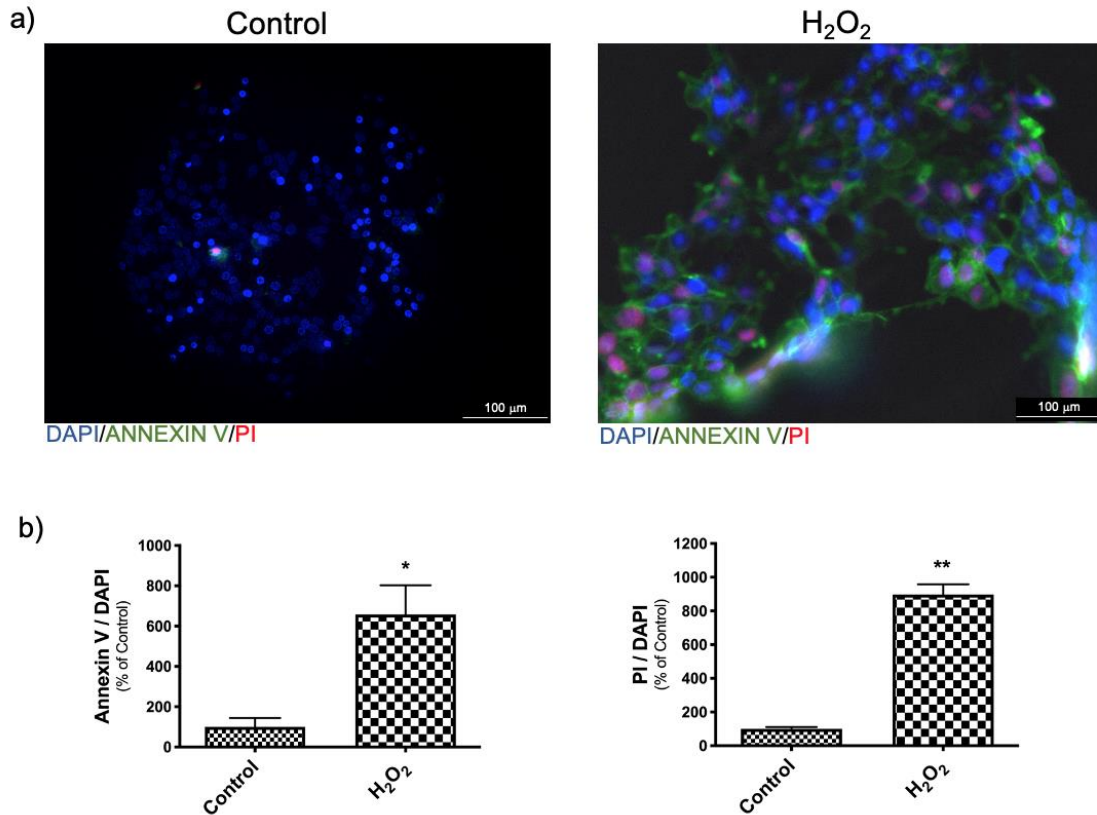


Figure 5.2 Representative images of DAPI, Annexin V-FITC and PI triple fluorescence staining showing cellular apoptosis after H_2O_2 treatment. DAPI: blue; Annexin V: green; PI: red. Histograms reports quantification of fluorescence of DAPI, Annexin V, and PI. The bars represent \pm the average \pm SD of independent experiments ($n = 3$). Statistically significant difference compared to control cells: * $p \leq 0.05$, ** $p \leq 0.01$.

To ascertain that EGb did not induce cell death, SK-N-BE cells were treated with various concentrations of EGb for 24 h. Results showed that EGb at all used concentrations did not reduce cell viability (**Fig 5.3**).



UNIONE EUROPEA
Fondo Sociale Europeo

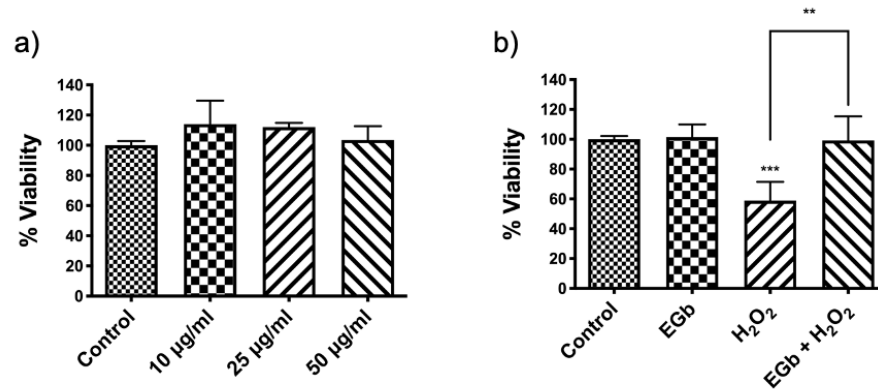


Figure 5.3 Effects of EGb on cell viability. Cell viability after treatments with different concentration of EGb. The bars represent \pm the average \pm SD of independent experiments ($n = 3$). Statistically significant difference compared to control cells: ** $p \leq 0.01$, *** $p \leq 0.005$.

To determine whether EGb played a role in protecting SK-N-BE from H₂O₂-induced cell death, cells were pre-treated for 24 h with EGb (25 µg/mL) and then challenged with H₂O₂ (75 µM) for the following 24 h. Analysis of cell vitality revealed that the oxidant sensitivity of SK-N-BE cells was completely reverted by pre-treatment with EGb (**Fig 5.4**).

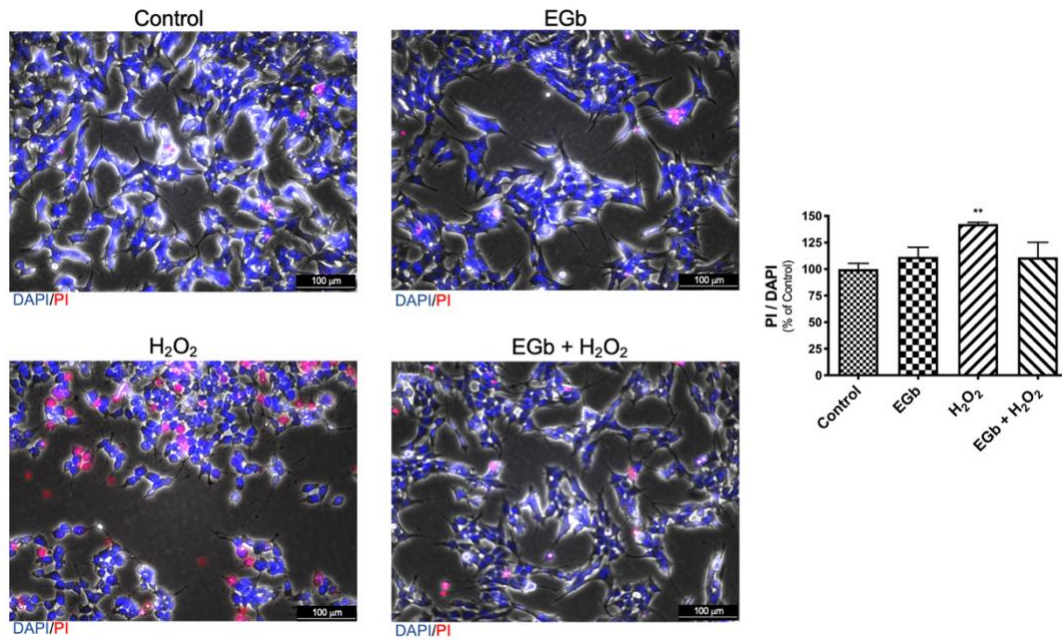


Figure 5.4 Cell viability after treatments with 25 mg/mL of EGb, 75 mM of H₂O₂ or a combination of them. Cells treated with DMSO were used as control. Fluorescent microscopic image of DAPI/PI stained cells; DAPI: blue; PI: red. Histogram reports quantification of fluorescence of DAPI and PI. The bars represent \pm the average \pm SD of independent experiments ($n = 3$). Statistically significant difference compared to control cells: ** $p \leq 0.01$

Concomitant addition of EGb and H₂O₂ or addition of EGb 24 h later H₂O₂ treatment did not result in a reversion of lethality. Results were confirmed by analysis with PI and DAPI staining, as shown by fluorescence microscopy analysis. Indeed, a comparable number of the PI positive cells were present in untreated, EGb treated and EGb- H₂O₂ treated cells, where a higher number were present in presence of H₂O₂ alone.



5.2. EGb Protects SK-N-BE Cells Against Oxidative Stress Induced Apoptosis

To confirm that EGb could protect cells against apoptotic cell death induced by oxidative stress, we first analysed the presence of poly(ADP-ribose) polymerase (PARP) cleavage, an hallmark of apoptosis. As expected, PARP cleavage increased after H₂O₂ treatment, although the cells were completely protected from oxidative stress-induced apoptosis in presence of EGb (**Fig 5.5**). Then, to study the protective mechanism of EGb against oxidative stress-induced apoptosis, we investigated the molecular signalling pathway involved in the apoptotic cell death analysing p53 expression.

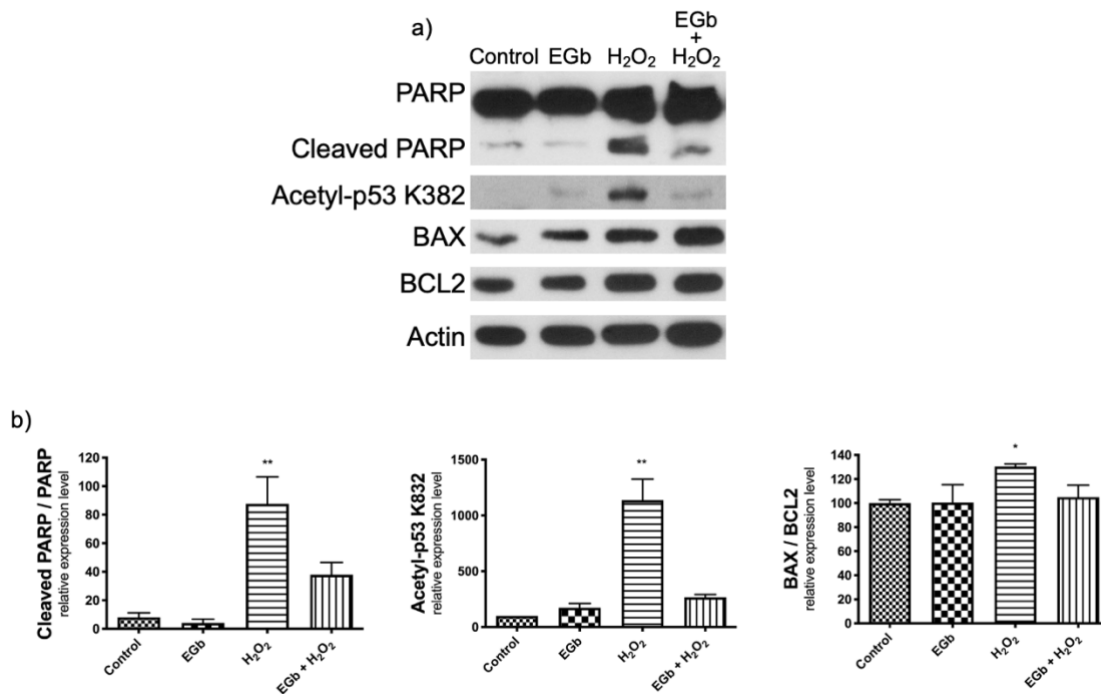


Figure 5.5 EGb protects SK-N-BE from apoptosis. Western blot analysis of protein expression of cleaved PARP, Acetylated-p53/K382, BAX and Bcl2 in SK-N-BE cells after treatments (a). expression of Acetylated-p53/K382, cleaved PARP and BAX/Bcl2



ratio normalized expression is reported in the histograms (b). β -Actin was used as loading control. The bars represent \pm the average \pm SD of independent experiments ($n = 3$). Statistically significant difference compared to control cells: * $p \leq 0.05$, ** $p \leq 0.01$.

Cells treated with DMSO were used as control.

The tumour suppressor protein p53, modulating cell homeostasis, has a determinant role in cell fate.

Oxidative stress, leading to post-translational modifications of p53, allows it to regulate genes that can activate cell survival or cell death processes [25].

Gene expression analysis, by q-PCR, revealed that p53 was not modulated by oxidative stress as well as by EGb (**Fig 5.6**).

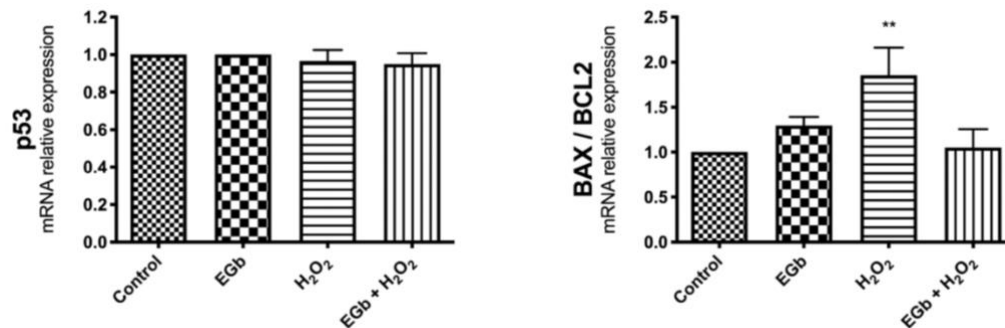


Figure 5.6 Quantitative analysis of mRNA expression levels of p53, BAX and Bcl-2 in SK-N-BE cells after treatments. Histograms report the expression of p53 and BAX/Bcl2 ratio. The bars represent \pm the average \pm SD of independent experiments ($n = 3$).

Statistically significant difference compared to control cells: ** $p \leq 0.01$. Cells treated with DMSO were used as control.

It is known that increased p53-acetylation at lysine 382 (K382) promotes p53-dependent pro-apoptotic activity in cancer cells [55]. Thus, we analysed by western blot analysis whether these post-translational modifications of



UNIONE EUROPEA
Fondo Sociale Europeo



p53 could account for the apoptotic reduction observed in presence of EGb. Results clearly demonstrate that K382 acetyl-p53 was strongly increased following H₂O₂ insult, however p53-acetylation was inhibited in presence of EGb (**Fig 5.5**).

Oxidative stress activates the mitochondrial intrinsic pathway of apoptosis [56]. p53, interacting with members of the Bcl-2 family, directly participating to the activation of the intrinsic apoptosis pathway [56]. We focused our attention on the ratio between two members of the Bcl-2 family, BAX and BCL-2, which are markers of cell susceptibility to intrinsic apoptosis. Protein expression analysis evidenced an increased BAX/Bcl-2 ratio in H₂O₂ treated SK-N-BE while pre-treatment with EGb restored a normal ratio (**Fig 5.5**). These results were also confirmed by gene expression analysis, by q-PCR of the corresponding genes (**Fig. 5.6**).

5.3. EGb mitigated the H₂O₂ induced decrease in mitochondrial membrane potential

Increased BAX/Bcl-2 ratio suggested that mitochondria are involved in apoptosis. Indeed, it is well known that, during intrinsic apoptosis, the mitochondrial membrane potential (MMP) collapses, triggering other downstream events in the apoptotic cascade. Thus, we investigated by JC-10 assay the change of MMP following H₂O₂ or EGb treatment of SK-N-BE cells. Results showed that untreated cells displayed intact, well-polarized mitochondria marked by a red punctate fluorescence. On contrary, H₂O₂ treated cells showed a reduction of the red fluorescence and an increase of the green one, indicating loss of MPM because of the progressive JC-10



UNIONE EUROPEA
Fondo Sociale Europeo



dislocation from mitochondria to the cytosol. On the contrary, EGb treatment restored the fluorescence to the values of untreated cells. (**Fig 5.7**).

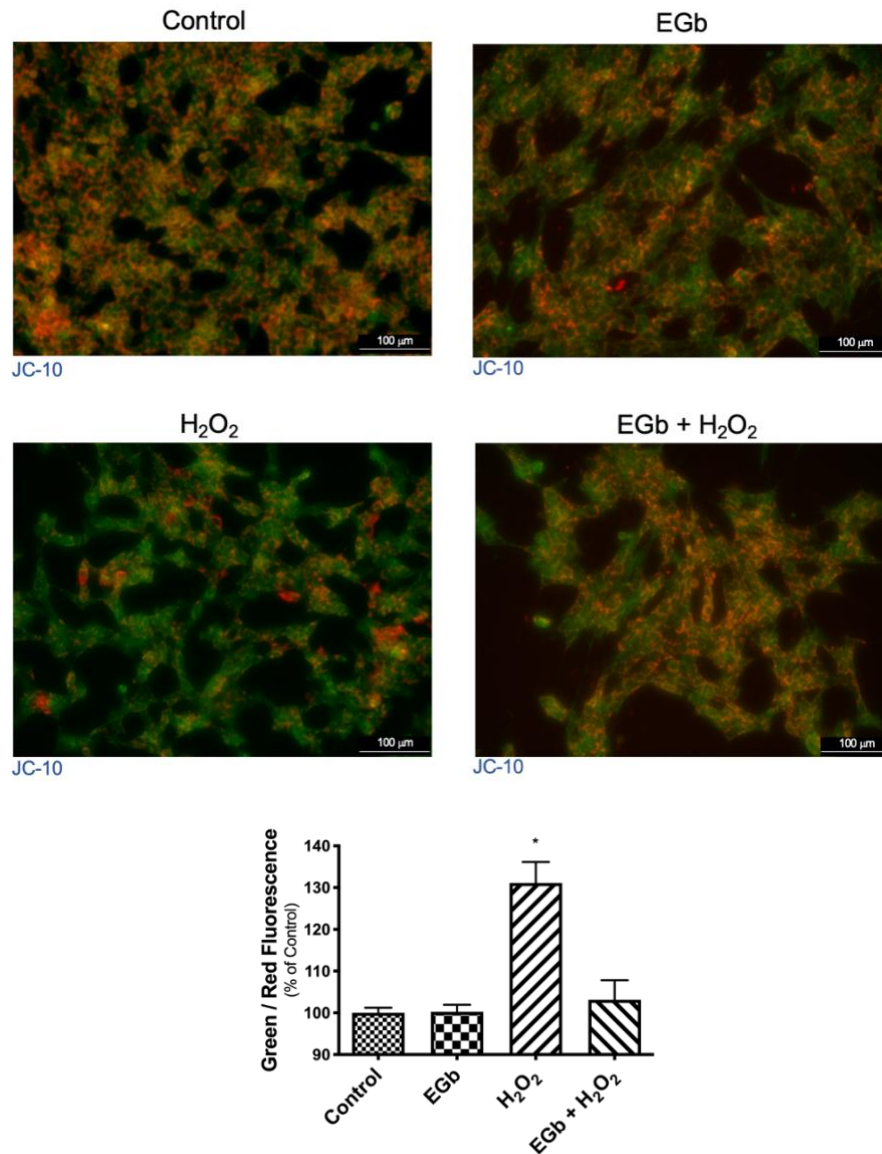


Figure 5.7 EGb reduces the decrease of mitochondrial membrane potential. Fluorescence analysis of mitochondria in control or EGb treated cells with or without H₂O₂. Histogram reports quantification of fluorescence of Red (540/570 nm) and green (485/534 nm). The bars represent \pm the average \pm SD of independent experiments ($n =$



UNIONE EUROPEA
Fondo Sociale Europeo



3). Statistically significant difference compared to control cells: * $p \leq 0.05$). Cells treated with DMSO were used as control.

5.4. EGb exhibits intracellular anti-apoptotic effect

To verify whether EGb acts as antioxidant into cells, or if it was able to directly scavenge H_2O_2 in the culture medium, SK-N-BE cells were treated for 24 h with EGb, then the culture medium was replaced and cells were challenged with H_2O_2 . Results showed that that EGb determined antioxidant protection on cell viability independently by its presence in the culture medium. In fact, pre-treatment with EGb was per se sufficient to attenuate the H_2O_2 -induced cell death in SK-N-BE cells (**Fig 5.8**).

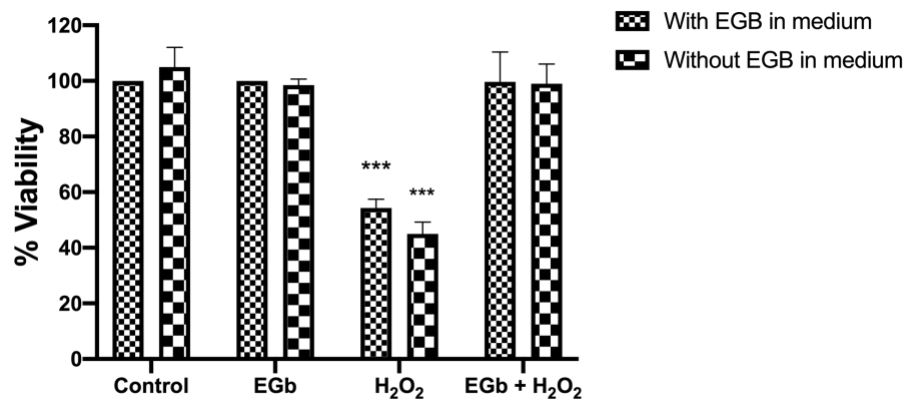


Figure 5.8 Intracellular effect of EGb. Cell viability analysis of SK-N-BE with or without EGb in the medium after H_2O_2 oxidative insult. The bars represent \pm the average \pm SD of independent experiments ($n = 3$). Statistically significant difference compared to control cells: *** $p \leq 0.005$). Cells treated with DMSO were used as control.

Moreover, in these conditions we observed a reduced cleavage of PARP protein, a reduced amount of K382 acetyl-p53 and a reduced BAX/Bcl-2 ratio



UNIONE EUROPEA
Fondo Sociale Europeo



(Fig 5.9), confirming that EGb was able to protect SNKBE cells by apoptotic cell death exerting an intracellular antioxidant action.

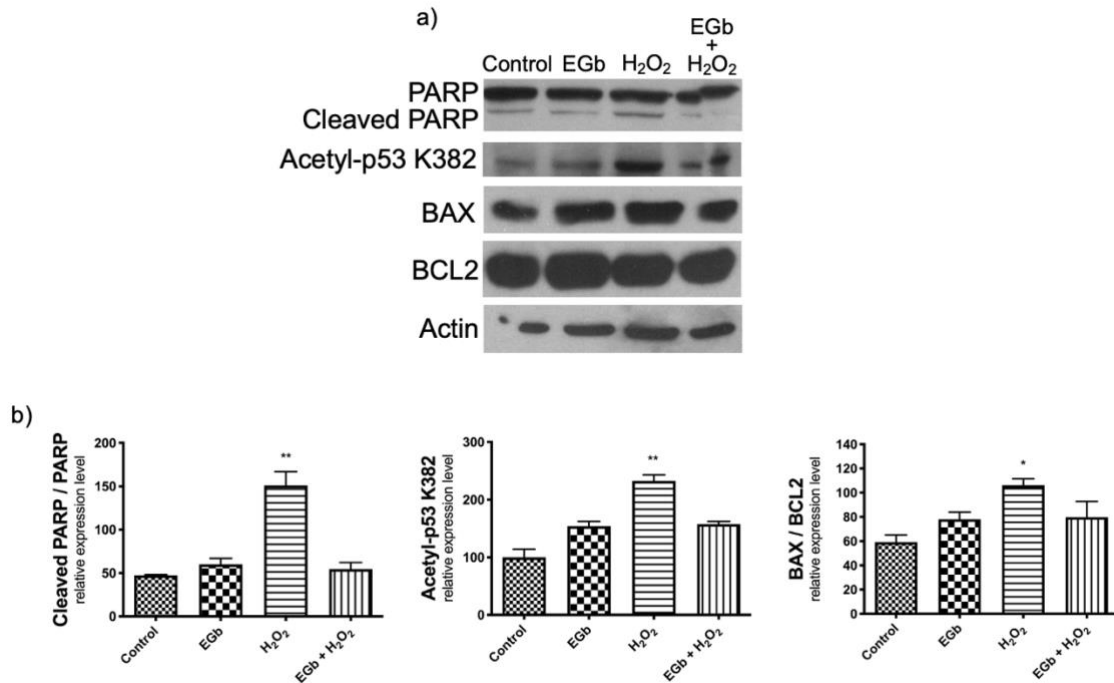


Figure 5.9 Protein expression analysis of cleaved PARP, Acetylated-p53/K382, BAX and Bcl2 in SK-N-BE cells after treatments by Western blot analysis (a). Histograms report the expression of Acetylated-p53/K382, cleaved PARP and BAX/Bcl2 ratio normalized expression (b). β -Actin was used as loading control. The bars represent \pm the average \pm SD of independent experiments ($n = 3$). Statistically significant difference compared to control cells: * $p \leq 0.05$, ** $p \leq 0.01$. Cells treated with DMSO were used as control.



UNIONE EUROPEA
Fondo Sociale Europeo



Discussion

The incidence of neurological disorders—the most dreaded maladies of older people—are expected to increase over the next few decades due to prolonged life expectancy [57]. To date, more than 1 in 10 individuals over 65 years are affected by neurodegenerative diseases and the numbers will continue to increase with age. Until now, no effective treatments have been described to cure these diseases and the costs for their management represent one of the leading medical and societal challenges faced by society [58]. For these reasons recent investigations have been focused to understanding their pathogenesis and to the development of novel therapeutics. *Ginkgo biloba*, a plant that has been used for thousands of years, is considered one of the more promising natural drugs. The extracts, obtained from *Ginkgo biloba* leaves, have been recently used also in clinical studies.

Most of the studies on the EGb concern its neuroprotective effects, against ageing. Standardized *Ginkgo biloba* extracts (EGb) have been used for treatment and prevention of different neurological disorders as Alzheimer's disease [21,22], Parkinson's disease [23,59], cerebral vascular deficit, and dementia [24,60].

Indeed, the brain is especially sensitive to the effects of ageing. This tissue being primarily composed of postmitotic cells—neurons and oligodendrocytes—is more vulnerable than proliferating cells to macromolecular damages, especially to DNA [61]. DNA damages in neurons accumulate from development throughout life. To escape this process, postmitotic neurons adopt selective mechanisms aimed to specifically repair genes actively transcribed [62].



UNIONE EUROPEA
Fondo Sociale Europeo



Oxidative stress is one of the main causes of neural damage. EGb exerts neuroprotective action mainly acting as free radical–scavenger. In fact, EGb is able to reduce the endogenous and the induced levels of ROS [63]. Moreover, EGb can directly upregulate antioxidant enzymes such as superoxide dismutase and catalase [64]. This activity is linked to the chemical structure of the flavonoids that allow to not only react and directly scavenge the hydroxyl radicals, but also to inhibit the formation of new hydroxyl radicals [65]. It is well known that oxidative stress determines the activation of the apoptotic processes, thus playing a pivotal role in most of neurological diseases. EGb can act on multiple cellular pathways with the final goal to balance the existing apoptotic machinery. In fact, EGb prevents mitochondrial membrane damage reducing the release of cytochrome c from the mitochondria, upregulates the antiapoptotic protein Bcl-2 and inhibits PARP cleavage [66].

The neuroprotective effect of EGb 761 has been reported in different neuronal cell lines in which it acts by inhibiting oxidative stress induced apoptosis [67-69] or the activation of mitochondrial intrinsic apoptosis [67,68]. A recent *in vivo* study reported that EGb 761 protected from brain injury by suppressing neuronal apoptosis [14]. Moreover, some studies reported the protective effect of *Ginkgo biloba* extract in people affected by neurodegenerative diseases [70,71].

In this study we analysed the protective effect of EGb on oxidative stress-induced apoptosis in SK-N-BE cells with the aim to unravel the molecular pathway in which EGb acts as antioxidant. Human neuroblastoma cell line N-type have neuronal morphology [72] and have been commonly used as



UNIONE EUROPEA
Fondo Sociale Europeo



model for research in neuroscience and in particular in studies related to oxidative stress and neurodegenerative diseases [33-35,73].

Our results demonstrated that the standardized extract EGb 761 significantly protected neuroblastoma cells from oxidative stress blocking apoptosis in a p53-dependent pathway. Interestingly, according to previous studies we found that EGB was able to inhibit p53 acetylation at lysine 382. It is known that p53 activity depends on the acetylation of specific lysine [74]. In addition, the acetylation of the C-terminal K382 lysine is crucial for p53 activation [75] since it results in the activation of PUMA promoter—a member of Bcl-2 family [76]. PUMA, promoting BAX multimerization and mitochondrial translocation, induces apoptosis [77]. Accordingly, our results show that EGb protects against mitochondrial membranes depolarization with a consequent reduction of BAX/Bcl-2 ratio. These results were supported by reduction of PARP cleavage with increased viability.

Previous studies reported that *Gingko biloba* extracts in cancer cells is able to induce apoptosis in a p53-dependent pathway by increasing the levels of p53 acetylation that, in turn, determines cell cycle arrest and apoptosis. On the contrary, our results demonstrated that the standardized extract EGb 761 significantly protected neuroblastoma cells from oxidative stress blocking apoptosis in a p53-dependent pathway. These results claim the different activity of EGb when used as neuroprotective or as anticancer drug [78].



UNIONE EUROPEA
Fondo Sociale Europeo



Conclusion

During this PhD period, my studies have demonstrated that hydro-alcoholic extracts of Aglianico and Falanghina grape seeds induce reduction of key tumorigenic characteristics of mesothelioma cells, such as viability, proliferation, and migration capacity. All the analysis performed determined that treatment with both extracts induces apoptosis in different mesothelioma cell lines via the intrinsic apoptosis pathway, by modulating proteins that regulate mitochondrial membrane permeability and by promoting cytochrome *c* leakage into the cytoplasm.

More interestingly, transcriptome analysis identified that the cholesterol biosynthesis pathway is the pathway most affected by Aglianico extract treatment and that it is linked to the p53-mediated apoptosis induction pathway.

AGS treatment also reduces cell viability and induces apoptosis in different tumour cell lines such as breast cancer and medulloblastoma cell lines. Also, in these cells a key role is represented by activation of the onco-suppressor p53 and by downregulation of its inhibitors, MDM2 and JUN.

As a continuation of the work, it would be important to test the efficacy of Aglianico extract also *in vivo* using a mouse tumour model. If the efficacy will be proved that it would be appropriate to fractionate the extract to identify the more active fraction responsible of the biological activity.



UNIONE EUROPEA
Fondo Sociale Europeo



Neurodegenerative disorders include a range of conditions that share common degenerative pathways, although they manifest clinical differences. Increased oxidative stress has been described in almost all neurodegenerative disorders. In neurons, imbalance between the accumulation of free radicals and antioxidant defences seems to be the link between cell death and progression of neurodegenerative diseases. Oxidative stress can trigger apoptosis in neuronal cells and excessive death of one or more populations of neurons, resulting in a neurodegenerative disease [79].

Our data suggest that EGb 761 blocking the onset of p53-dependent apoptotic pathway induced by oxidative stress, could be considered as antioxidant nutraceutical to be potentially used for the prevention and treatment of neurodegenerative diseases. This hypothesis could be strengthened with a larger number of randomized clinical trials.

These studies unravel two possible uses of polyphenols. In fact, if grape seed extracts are able to induce apoptosis in cancer cells, on the other hand polyphenols of different origin, as those extracted from *Ginkgo biloba* leaves, are able to reduce the effects of oxidative stress and could prevent neurodegenerative diseases.

Polyphenols of natural origin are many and can have very different actions. This is the reason why they represent a good future perspective for the treatment of many diseases and disorders. Moreover, they are safe and have a very low toxicity, so, it is easy to test their efficacy in pre-clinical and clinical studies.



UNIONE EUROPEA
Fondo Sociale Europeo



References

1. Di Meo, F.; Donato, S.; Di Pardo, A.; Maglione, V.; Filosa, S.; Crispi, S. New Therapeutic Drugs from Bioactive Natural Molecules: The Role of Gut Microbiota Metabolism in Neurodegenerative Diseases. *Curr Drug Metab* **2018**, *19*, 478-489, doi:10.2174/1389200219666180404094147.
2. Di Meo, F.; Margarucci, S.; Galderisi, U.; Crispi, S.; Peluso, G. Curcumin, Gut Microbiota, and Neuroprotection. *Nutrients* **2019**, *11*, doi:10.3390/nu11102426.
3. Di Meo, F.; Cuciniello, R.; Margarucci, S.; Bergamo, P.; Petillo, O.; Peluso, G.; Filosa, S.; Crispi, S. Prevents Oxidative Stress-Induced Apoptosis Blocking p53 Activation in Neuroblastoma Cells. *Antioxidants (Basel)* **2020**, *9*, doi:10.3390/antiox9040279.
4. Hosu, A.; Cristea, V.M.; Cimpoi, C. Analysis of total phenolic, flavonoids, anthocyanins and tannins content in Romanian red wines: prediction of antioxidant activities and classification of wines using artificial neural networks. *Food Chem* **2014**, *150*, 113-118, doi:10.1016/j.foodchem.2013.10.153.
5. Khoo, H.E.; Azlan, A.; Tang, S.T.; Lim, S.M. Anthocyanidins and anthocyanins: colored pigments as food, pharmaceutical ingredients, and the potential health benefits. *Food Nutr Res* **2017**, *61*, 1361779, doi:10.1080/16546628.2017.1361779.
6. Weidner, S.; Rybarczyk, A.; Karamać, M.; Król, A.; Mostek, A.; Grębosz, J.; Amarowicz, R. Differences in the phenolic composition and antioxidant properties between *Vitis coignetiae* and *Vitis vinifera* seeds extracts. *Molecules* **2013**, *18*, 3410-3426, doi:10.3390/molecules18033410.
7. Xia, E.Q.; Deng, G.F.; Guo, Y.J.; Li, H.B. Biological activities of polyphenols from grapes. *Int J Mol Sci* **2010**, *11*, 622-646, doi:10.3390/ijms11020622.



UNIONE EUROPEA
Fondo Sociale Europeo



8. Higgins, J.A.; Zainol, M.; Brown, K.; Jones, G.D. Anthocyanins as tertiary chemopreventive agents in bladder cancer: anti-oxidant mechanisms and interaction with mitomycin C. *Mutagenesis* **2014**, *29*, 227-235, doi:10.1093/mutage/geu009.
9. Márquez Campos, E.; Stehle, P.; Simon, M.C. Microbial Metabolites of Flavan-3-Ols and Their Biological Activity. *Nutrients* **2019**, *11*, doi:10.3390/nu11102260.
10. Teng, H.; Chen, L. Polyphenols and bioavailability: an update. *Crit Rev Food Sci Nutr* **2019**, *59*, 2040-2051, doi:10.1080/10408398.2018.1437023.
11. Aslam, S.; Jahan, N.; Rahman, K.; Zafar, F.; Ashraf, M.Y. Synergistic interactions of polyphenols and their effect on antiradical potential. *Pak J Pharm Sci* **2017**, *30*, 1297-1304.
12. Nandakumar, V.; Singh, T.; Katiyar, S.K. Multi-targeted prevention and therapy of cancer by proanthocyanidins. *Cancer Lett* **2008**, *269*, 378-387, doi:10.1016/j.canlet.2008.03.049.
13. Mittal, A.; Elmets, C.A.; Katiyar, S.K. Dietary feeding of proanthocyanidins from grape seeds prevents photocarcinogenesis in SKH-1 hairless mice: relationship to decreased fat and lipid peroxidation. *Carcinogenesis* **2003**, *24*, 1379-1388, doi:10.1093/carcin/bgg095.
14. Yu, T.; Fan, Y.; Xu, Y.; Xu, L.; Xu, G.; Cao, F.; Jiang, H. Standardized Ginkgo biloba extract EGb 761(R) attenuates early brain injury following subarachnoid hemorrhage via suppressing neuronal apoptosis through the activation of Akt signaling. *Biomed Pharmacother* **2018**, *107*, 329-337, doi:10.1016/j.biopha.2018.08.012.
15. Zhou, G.; Ma, J.; Tang, Y.; Wang, X.; Zhang, J.; Duan, J.A. Multi-Response Optimization of Ultrasonic Assisted Enzymatic Extraction Followed by Macroporous Resin Purification for Maximal Recovery of Flavonoids and Ginkgolides from Waste. *Molecules* **2018**, *23*, doi:10.3390/molecules23051029.



UNIONE EUROPEA
Fondo Sociale Europeo



16. Chávez-Morales, R.M.; Jaramillo-Juárez, F.; Rodríguez-Vázquez, M.L.; Martínez-Saldaña, M.C.; Del Río, F.A.P.; Garfias-López, J.A. The Ginkgo biloba extract (GbE) protects the kidney from damage produced by a single and low dose of carbon tetrachloride in adult male rats. *Exp Toxicol Pathol* **2017**, *69*, 430-434, doi:10.1016/j.etp.2017.04.003.
17. Eckert, A.; Keil, U.; Scherping, I.; Hauptmann, S.; Muller, W.E. Stabilization of mitochondrial membrane potential and improvement of neuronal energy metabolism by Ginkgo biloba extract EGb 761. *Ann N Y Acad Sci* **2005**, *1056*, 474-485, doi:10.1196/annals.1352.023.
18. Chen, C.; Wei, T.; Gao, Z.; Zhao, B.; Hou, J.; Xu, H.; Xin, W.; Packer, L. Different effects of the constituents of EGb761 on apoptosis in rat cerebellar granule cells induced by hydroxyl radicals. *Biochem Mol Biol Int* **1999**, *47*, 397-405, doi:10.1080/15216549900201423.
19. Gohil, K.; Packer, L. Bioflavonoid-rich botanical extracts show antioxidant and gene regulatory activity. *Ann N Y Acad Sci* **2002**, *957*, 70-77, doi:10.1111/j.1749-6632.2002.tb02906.x.
20. Zhou, H.C.; Tam, N.F.Y.; Lin, Y.M.; Ding, Z.H.; Chai, W.M.; Wei, S.D. Relationships between Degree of Polymerization and Antioxidant Activities: A Study on Proanthocyanidins from the Leaves of a Medicinal Mangrove Plant *Ceriops tagal*. *Plos One* **2014**, *9*, doi:ARTN e107606
10.1371/journal.pone.0107606.
21. Rapp, M.; Burkart, M.; Kohlmann, T.; Bohlken, J. Similar treatment outcomes with Ginkgo biloba extract EGb 761 and donepezil in Alzheimer's dementia in very old age: A retrospective observational study. *Int J Clin Pharmacol Ther* **2018**, *56*, 130-133, doi:10.5414/CP203103.
22. Kaur, N.; Dhiman, M.; Perez-Polo, J.R.; Mantha, A.K. Ginkgolide B revamps neuroprotective role of apurinic/aprimidinic endonuclease 1 and mitochondrial oxidative phosphorylation against Abeta25-35 - induced neurotoxicity in human neuroblastoma cells. *J Neurosci Res* **2015**, *93*, 938-947, doi:10.1002/jnr.23565.



UNIONE EUROPEA
Fondo Sociale Europeo



23. Vijayakumaran, S.; Nakamura, Y.; Henley, J.M.; Pountney, D.L. Ginkgolic acid promotes autophagy-dependent clearance of intracellular alpha-synuclein aggregates. *Mol Cell Neurosci* **2019**, *101*, 103416, doi:10.1016/j.mcn.2019.103416.
24. Kandiah, N.; Ong, P.A.; Yuda, T.; Ng, L.L.; Mamun, K.; Merchant, R.A.; Chen, C.; Dominguez, J.; Marasigan, S.; Ampil, E.; et al. Treatment of dementia and mild cognitive impairment with or without cerebrovascular disease: Expert consensus on the use of Ginkgo biloba extract, EGb 761((R)). *CNS Neurosci Ther* **2019**, *25*, 288-298, doi:10.1111/cns.13095.
25. Beyfuss, K.; Hood, D.A. A systematic review of p53 regulation of oxidative stress in skeletal muscle. *Redox Rep* **2018**, *23*, 100-117, doi:10.1080/13510002.2017.1416773.
26. Carbone, M.; Adusumilli, P.S.; Alexander, H.R.; Baas, P.; Bardelli, F.; Bononi, A.; Bueno, R.; Felley-Bosco, E.; Galateau-Salle, F.; Jablons, D.; et al. Mesothelioma: Scientific clues for prevention, diagnosis, and therapy. *CA Cancer J Clin* **2019**, *69*, 402-429, doi:10.3322/caac.21572.
27. Harbeck, N.; Gnant, M. Breast cancer. *Lancet* **2017**, *389*, 1134-1150, doi:10.1016/S0140-6736(16)31891-8.
28. Anastasiadi, Z.; Lianos, G.D.; Ignatiadou, E.; Harissis, H.V.; Mitsis, M. Breast cancer in young women: an overview. *Updates Surg* **2017**, *69*, 313-317, doi:10.1007/s13304-017-0424-1.
29. Huang, Z.; Yu, P.; Tang, J. Characterization of Triple-Negative Breast Cancer MDA-MB-231 Cell Spheroid Model. *Onco Targets Ther* **2020**, *13*, 5395-5405, doi:10.2147/OTT.S249756.
30. Ostrom, Q.T.; Patil, N.; Cioffi, G.; Waite, K.; Kruchko, C.; Barnholtz-Sloan, J.S. Corrigendum to: CBTRUS Statistical Report: Primary Brain and Other Central Nervous System Tumors Diagnosed in the United States in 2013-2017. *Neuro Oncol* **2020**, doi:10.1093/neuonc/noaa269.



UNIONE EUROPEA
Fondo Sociale Europeo



31. Bergamini, C.M.; Gambetti, S.; Dondi, A.; Cervellati, C. Oxygen, reactive oxygen species and tissue damage. *Curr Pharm Des* **2004**, *10*, 1611-1626, doi:10.2174/1381612043384664.
32. Filosa, S.; Pecorelli, A.; D'Esposito, M.; Valacchi, G.; Hajek, J. Exploring the possible link between MeCP2 and oxidative stress in Rett syndrome. *Free Radic Biol Med* **2015**, *88*, 81-90, doi:10.1016/j.freeradbiomed.2015.04.019.
33. Krishna, A.; Biryukov, M.; Trefois, C.; Antony, P.M.; Hussong, R.; Lin, J.; Heinaniemi, M.; Glusman, G.; Koglsberger, S.; Boyd, O.; et al. Systems genomics evaluation of the SH-SY5Y neuroblastoma cell line as a model for Parkinson's disease. *BMC Genomics* **2014**, *15*, 1154, doi:10.1186/1471-2164-15-1154.
34. Mata, I.F.; Jang, Y.; Kim, C.H.; Hanna, D.S.; Dorschner, M.O.; Samii, A.; Agarwal, P.; Roberts, J.W.; Klepitskaya, O.; Shprecher, D.R.; et al. The RAB39B p.G192R mutation causes X-linked dominant Parkinson's disease. *Mol Neurodegener* **2015**, *10*, 50, doi:10.1186/s13024-015-0045-4.
35. Maraldi, T.; Riccio, M.; Zambonin, L.; Vinceti, M.; De Pol, A.; Hakim, G. Low levels of selenium compounds are selectively toxic for a human neuron cell line through ROS/RNS increase and apoptotic process activation. *Neurotoxicology* **2011**, *32*, 180-187, doi:10.1016/j.neuro.2010.10.008.
36. Crispi, S.; Calogero, R.A.; Santini, M.; Mellone, P.; Vincenzi, B.; Citro, G.; Vicidomini, G.; Fasano, S.; Meccariello, R.; Cobellis, G.; et al. Global Gene Expression Profiling Of Human Pleural Mesotheliomas: Identification of Matrix Metalloproteinase 14 (MMP-14) as Potential Tumour Target. *Plos One* **2009**, *4*, doi:ARTN e7016 10.1371/journal.pone.0007016.
37. Baldi, A.; Piccolo, M.T.; Boccellino, M.R.; Donizetti, A.; Cardillo, I.; La Porta, R.; Quagliuolo, L.; Spugnini, E.P.; Cordero, F.; Citro, G.; et al. Apoptosis Induced by Piroxicam plus Cisplatin Combined Treatment Is Triggered by p21 in Mesothelioma. *Plos One* **2011**, *6*, doi:ARTN e23569



UNIONE EUROPEA
Fondo Sociale Europeo



10.1371/journal.pone.0023569.

38. Fischer, U.; Janicke, R.U.; Schulze-Osthoff, K. Many cuts to ruin: a comprehensive update of caspase substrates. *Cell Death Differ* **2003**, *10*, 76-100, doi:10.1038/sj.cdd.4401160.
39. Di Meo, F.; Aversano, R.; Diretto, G.; Demurtas, O.; Villano, C.; Cozzolino, S.; Filosa, S.; Carputo, D.; Crisp, S. Anti-cancer activity of grape seed semi-polar extracts in human mesothelioma cell lines. *Journal of Functional Foods* **2019**, *61*.
40. Wang, Y.; Lee, K.W.; Chan, F.L.; Chen, S.A.; Leung, L.K. The red wine polyphenol resveratrol displays bilevel inhibition on aromatase in breast cancer cells. *Toxicological Sciences* **2006**, *92*, 71-77, doi:10.1093/toxsci/kfj190.
41. Mantena, S.K.; Baliga, M.S.; Katiyar, S.K. Grape seed proanthocyanidins induce apoptosis and inhibit metastasis of highly metastatic breast carcinoma cells. *Carcinogenesis* **2006**, *27*, 1682-1691, doi:10.1093/carcin/bgl030.
42. Chou, S.C.; Kaur, M.; Thompson, J.A.; Agarwal, R.; Agarwal, C. Influence of Gallate Esterification on the Activity of Procyanidin B2 in Androgen-Dependent Human Prostate Carcinoma LNCaP Cells. *Pharmaceutical Research* **2010**, *27*, 619-627, doi:10.1007/s11095-009-0037-6.
43. Mitsuhashi, S.; Saito, A.; Nakajima, N.; Shima, H.; Ubukata, M. Pyrogallol structure in polyphenols is involved in apoptosis-induction on HEK293T and K562 cells. *Molecules* **2008**, *13*, 2998-3006, doi:10.3390/molecules13122998.
44. Cheah, K.Y.; Howarth, G.S.; Bindon, K.A.; Kennedy, J.A.; Bastian, S.E. Low molecular weight procyanidins from grape seeds enhance the impact of 5-Fluorouracil chemotherapy on Caco-2 human colon cancer cells. *PLoS One* **2014**, *9*, e98921, doi:10.1371/journal.pone.0098921.
45. Moll, U.M.; Petrenko, O. The MDM2-p53 interaction. *Mol Cancer Res* **2003**, *1*, 1001-1008.



46. Momand, J.; Jung, D.; Wilczynski, S.; Niland, J. The MDM2 gene amplification database. *Nucleic Acids Res* **1998**, *26*, 3453-3459, doi:10.1093/nar/26.15.3453.
47. Onel, K.; Cordon-Cardo, C. MDM2 and prognosis. *Mol Cancer Res* **2004**, *2*, 1-8.
48. Ware, P.L.; Snow, A.N.; Gvalani, M.; Pettenati, M.J.; Qasem, S.A. MDM2 copy numbers in well-differentiated and dedifferentiated liposarcoma: characterizing progression to high-grade tumors. *Am J Clin Pathol* **2014**, *141*, 334-341, doi:10.1309/AJCPLYU89XHSNHQO.
49. Schreiber, M.; Kolbus, A.; Piu, F.; Szabowski, A.; Möhle-Steinlein, U.; Tian, J.; Karin, M.; Angel, P.; Wagner, E.F. Control of cell cycle progression by c-Jun is p53 dependent. *Genes Dev* **1999**, *13*, 607-619, doi:10.1101/gad.13.5.607.
50. Waterham, H.R.; Koster, J.; Romeijn, G.J.; Hennekam, R.C.; Vreken, P.; Andersson, H.C.; FitzPatrick, D.R.; Kelley, R.I.; Wanders, R.J. Mutations in the 3beta-hydroxysterol Delta24-reductase gene cause desmosterolosis, an autosomal recessive disorder of cholesterol biosynthesis. *Am J Hum Genet* **2001**, *69*, 685-694, doi:10.1086/323473.
51. Tsukiyama-Kohara, K. Role of oxidative stress in hepatocarcinogenesis induced by hepatitis C virus. *Int J Mol Sci* **2012**, *13*, 15271-15278, doi:10.3390/ijms131115271.
52. Nishimura, T.; Kohara, M.; Izumi, K.; Kasama, Y.; Hirata, Y.; Huang, Y.; Shuda, M.; Mukaidani, C.; Takano, T.; Tokunaga, Y.; et al. Hepatitis C virus impairs p53 via persistent overexpression of 3beta-hydroxysterol Delta24-reductase. *J Biol Chem* **2009**, *284*, 36442-36452, doi:10.1074/jbc.M109.043232.
53. Qin, J.J.; Li, X.; Hunt, C.; Wang, W.; Wang, H.; Zhang, R. Natural products targeting the p53-MDM2 pathway and mutant p53: Recent advances and implications in cancer medicine. *Genes Dis* **2018**, *5*, 204-219, doi:10.1016/j.gendis.2018.07.002.



UNIONE EUROPEA
Fondo Sociale Europeo



54. Crispi, S.; Cardillo, I.; Spugnini, E.P.; Citro, G.; Menegozzo, S.; Baldi, A. Biological agents involved in malignant mesothelioma: relevance as biomarkers or therapeutic targets. *Curr Cancer Drug Targets* **2010**, *10*, 19-26.
55. Reed, S.M.; Quelle, D.E. p53 Acetylation: Regulation and Consequences. *Cancers (Basel)* **2014**, *7*, 30-69, doi:10.3390/cancers7010030.
56. Redza-Dutordoir, M.; Averill-Bates, D.A. Activation of apoptosis signalling pathways by reactive oxygen species. *Biochim Biophys Acta* **2016**, *1863*, 2977-2992, doi:10.1016/j.bbamcr.2016.09.012.
57. Wyss-Coray, T. Ageing, neurodegeneration and brain rejuvenation. *Nature* **2016**, *539*, 180-186, doi:10.1038/nature20411.
58. Hou, Y.; Dan, X.; Babbar, M.; Wei, Y.; Hasselbalch, S.G.; Croteau, D.L.; Bohr, V.A. Ageing as a risk factor for neurodegenerative disease. *Nat Rev Neurol* **2019**, *15*, 565-581, doi:10.1038/s41582-019-0244-7.
59. Rojas, P.; Montes, P.; Rojas, C.; Serrano-Garcia, N.; Rojas-Castaneda, J.C. Effect of a phytopharmaceutical medicine, Ginkgo biloba extract 761, in an animal model of Parkinson's disease: therapeutic perspectives. *Nutrition* **2012**, *28*, 1081-1088, doi:10.1016/j.nut.2012.03.007.
60. Spiegel, R.; Kalla, R.; Mantokoudis, G.; Maire, R.; Mueller, H.; Hoerr, R.; Ihl, R. Ginkgo biloba extract EGb 761((R)) alleviates neurosensory symptoms in patients with dementia: a meta-analysis of treatment effects on tinnitus and dizziness in randomized, placebo-controlled trials. *Clin Interv Aging* **2018**, *13*, 1121-1127, doi:10.2147/CIA.S157877.
61. Madabhushi, R.; Pan, L.; Tsai, L.H. DNA damage and its links to neurodegeneration. *Neuron* **2014**, *83*, 266-282, doi:10.1016/j.neuron.2014.06.034.
62. Chow, H.M.; Herrup, K. Genomic integrity and the ageing brain. *Nat Rev Neurosci* **2015**, *16*, 672-684, doi:10.1038/nrn4020.



UNIONE EUROPEA
Fondo Sociale Europeo



63. Smith, J.V.; Luo, Y. Studies on molecular mechanisms of Ginkgo biloba extract. *Appl Microbiol Biotechnol* **2004**, *64*, 465-472, doi:10.1007/s00253-003-1527-9.
64. Bridi, R.; Crossetti, F.P.; Steffen, V.M.; Henriques, A.T. The antioxidant activity of standardized extract of Ginkgo biloba (EGb 761) in rats. *Phytother Res* **2001**, *15*, 449-451, doi:10.1002/ptr.814.
65. Zimmermann, M.; Colciaghi, F.; Cattabeni, F.; Di Luca, M. Ginkgo biloba extract: from molecular mechanisms to the treatment of Alzheimer's disease. *Cell Mol Biol (Noisy-le-grand)* **2002**, *48*, 613-623.
66. Smith, J.V.; Burdick, A.J.; Golik, P.; Khan, I.; Wallace, D.; Luo, Y. Anti-apoptotic properties of Ginkgo biloba extract EGb 761 in differentiated PC12 cells. *Cellular and Molecular Biology* **2002**, *48*, 699-707.
67. Shi, C.; Zhao, L.; Zhu, B.; Li, Q.; Yew, D.T.; Yao, Z.; Xu, J. Dosage effects of EGb761 on hydrogen peroxide-induced cell death in SH-SY5Y cells. *Chem Biol Interact* **2009**, *180*, 389-397, doi:10.1016/j.cbi.2009.04.008.
68. Jiang, X.; Nie, B.; Fu, S.; Hu, J.; Yin, L.; Lin, L.; Wang, X.; Lu, P.; Xu, X.M. EGb761 protects hydrogen peroxide-induced death of spinal cord neurons through inhibition of intracellular ROS production and modulation of apoptotic regulating genes. *J Mol Neurosci* **2009**, *38*, 103-113, doi:10.1007/s12031-008-9140-0.
69. Ni, Y.; Zhao, B.; Hou, J.; Xin, W. Preventive effect of Ginkgo biloba extract on apoptosis in rat cerebellar neuronal cells induced by hydroxyl radicals. *Neurosci Lett* **1996**, *214*, 115-118, doi:10.1016/0304-3940(96)12897-4.
70. Savaskan, E.; Mueller, H.; Hoerr, R.; von Gunten, A.; Gauthier, S. Treatment effects of Ginkgo biloba extract EGb 761® on the spectrum of behavioral and psychological symptoms of dementia: meta-analysis of randomized controlled trials. *Int Psychogeriatr* **2018**, *30*, 285-293, doi:10.1017/S1041610217001892.



UNIONE EUROPEA
Fondo Sociale Europeo



71. Gauthier, S.; Schlaefke, S. Efficacy and tolerability of Ginkgo biloba extract EGb 761® in dementia: a systematic review and meta-analysis of randomized placebo-controlled trials. *Clin Interv Aging* **2014**, *9*, 2065-2077, doi:10.2147/CIA.S72728.
72. Corey, J.M.; Gertz, C.C.; Sutton, T.J.; Chen, Q.; Mycek, K.B.; Wang, B.S.; Martin, A.A.; Johnson, S.L.; Feldman, E.L. Patterning N-type and S-type neuroblastoma cells with Pluronic F108 and ECM proteins. *J Biomed Mater Res A* **2010**, *93*, 673-686, doi:10.1002/jbm.a.32485.
73. Testa, G.; Staurenghi, E.; Giannelli, S.; Gargiulo, S.; Guglielmotto, M.; Tabaton, M.; Tamagno, E.; Gamba, P.; Leonarduzzi, G. A silver lining for 24-hydroxycholesterol in Alzheimer's disease: The involvement of the neuroprotective enzyme sirtuin 1. *Redox Biol* **2018**, *17*, 423-431, doi:10.1016/j.redox.2018.05.009.
74. Knights, C.D.; Catania, J.; Di Giovanni, S.; Muratoglu, S.; Perez, R.; Swartzbeck, A.; Quong, A.A.; Zhang, X.; Beerman, T.; Pestell, R.G.; et al. Distinct p53 acetylation cassettes differentially influence gene-expression patterns and cell fate. *J Cell Biol* **2006**, *173*, 533-544, doi:10.1083/jcb.200512059.
75. Olsson, A.; Manzl, C.; Strasser, A.; Villunger, A. How important are post-translational modifications in p53 for selectivity in target-gene transcription and tumour suppression? *Cell Death Differ* **2007**, *14*, 1561-1575, doi:10.1038/sj.cdd.4402196.
76. Brochier, C.; Dennis, G.; Riviaccio, M.A.; McLaughlin, K.; Coppola, G.; Ratan, R.R.; Langley, B. Specific acetylation of p53 by HDAC inhibition prevents DNA damage-induced apoptosis in neurons. *J Neurosci* **2013**, *33*, 8621-8632, doi:10.1523/JNEUROSCI.5214-12.2013.
77. Ming, L.; Wang, P.; Bank, A.; Yu, J.; Zhang, L. PUMA Dissociates Bax and Bcl-X(L) to induce apoptosis in colon cancer cells. *J Biol Chem* **2006**, *281*, 16034-16042, doi:10.1074/jbc.M513587200.



UNIONE EUROPEA
Fondo Sociale Europeo



78. Park, H.J.; Kim, M.M. Flavonoids in Ginkgo biloba fallen leaves induce apoptosis through modulation of p53 activation in melanoma cells. *Oncol Rep* **2015**, *33*, 433-438, doi:10.3892/or.2014.3602.
79. Mattson, M.P. Apoptosis in neurodegenerative disorders. *Nat Rev Mol Cell Biol* **2000**, *1*, 120-129, doi:10.1038/35040009.



UNIONE EUROPEA
Fondo Sociale Europeo



Dott. Francesco Di Meo peer reviewed papers published during the PhD period:

- 1) Di Meo F, Valentino A, Petillo O, Peluso G, Filosa S, Crispi S. Bioactive Polyphenols and Neuromodulation: Molecular Mechanisms in Neurodegeneration. *Int J Mol Sci.* 2020 Apr 7;21(7):2564. doi: 10.3390/ijms21072564.
- 2) Di Meo F, Cuciniello R, Margarucci S, Bergamo P, Petillo O, Peluso G, Filosa S, Crispi S. Ginkgo biloba Prevents Oxidative Stress-Induced Apoptosis Blocking p53 Activation in Neuroblastoma Cells. *Antioxidants (Basel).* 2020 Mar 26;9(4):279. doi: 10.3390/antiox9040279.
- 3) Di Meo F, Margarucci S, Galderisi U, Crispi S, Peluso G. Curcumin, Gut Microbiota, and Neuroprotection. *Nutrients.* 2019 Oct 11;11(10):2426. doi: 10.3390/nu11102426.
- 4) Di Meo F, Aversano R, Diretto G, Demurtas O, Villano C, Cozzolino S, Filosa S, Carputo D, Crispi S. Anti-cancer activity of grape seed semi-polar extracts in human mesothelioma cell lines. *Journal of Functional Foods.* October 2019, 103515. DOI: 10.1016/j.jff.2019.103515
- 5) Di Meo F, Filosa S, Madonna M, Giello G, Di Pardo A, Maglione V, Baldi A, Crispi S. Curcumin C3 complex®/Bioperine® has antineoplastic activity in mesothelioma: an in vitro and in vivo analysis. *J Exp Clin Cancer Res.* 2019 Aug 16;38(1):360. doi: 10.1186/s13046-019-1368-8.



UNIONE EUROPEA
Fondo Sociale Europeo



- 6) Di Meo F, Donato S, Di Pardo A, Maglione V, Filosa S, Crispi S. New Therapeutic Drugs from Bioactive Natural Molecules: The Role of Gut Microbiota Metabolism in Neurodegenerative Diseases. *Curr Drug Metab.* 2018;19(6):478-489. doi: 10.2174/1389200219666180404094147.
- 7) Filosa S, Di Meo F, Crispi S. Polyphenols-gut microbiota interplay and brain neuromodulation. *Neural Regen Res.* 2018 Dec;13(12):2055-2059. doi: 10.4103/1673-5374.241429.